筑 波 大 学

博 士 (医学) 学 位 論 文

Function of the Small G Protein Arf6 in Lymphangiogenesis

（リンパ管新生における低分子量 G タンパク質 Arf6 の機能）

２０１７

筑波大学大学院 博士課程 人間総合科学研究科

林　岳謙

Abbreviations

ACAP, Arf GAP with coiled-coil, ankyrin repeat and PH domains

ADAP, Arf6 GAP with dual PH domains

AGAP, Arf GAP with GTP-binding protein-like, ankyrin repeat and PH domains

AGFG, Arf6 GAP with FG repeats-containing domain

AP-2, adaptor protein complex-2

ARAP, Arf GAP with Rho-GAP, ankyrin repeat and PH domains

Arf6, ADP-ribosylation factor 6

$Arf6^{-/-}$, $Arf6$ knockout

ARL, Arf-like

ARP, Arf-related protein

ARNO, Arf nucleotide binding site opener

ASAP, Arf GAP with SH3, ankyrin repeat and PH domains

BFA, brefeldin A

BRAG, BFA resistant Arf-guanine nucleotide exchange factor

BIG, brefeldin A-inhibited GEF

CCBE1, collagen and calcium binding EGF domains 1

CIE, clathrin-independent endocytosis

cKO, conditional knockout

CLECL-2, C-type lectin receptor 2

EFA6, exchange factor for Arf6

ECM, cell-extracellular matrix

EGFR, epidermal growth factor receptor

EMT, epithelial-mesenchymal transition

ERK, extracellular signal-regulated kinase

FcR, Fc receptor

FOXC2, forkhead box protein C2

GAP, GTPase-activating protein

GBF1, Golgi-specific brefeldin A-resistant Arf-guanine nucleotide exchange factor 1

GEF, guanine exchange factor

GEP100, Arf-guanine nucleotide exchange protein 100

GGA3, Golgi-localized, gamma adaptin ear-containing, Arf-binding protein 3

GIT, GRK interactor

GPCR, G-protein-coupled receptor

GRP1, general receptor of phosphoinositides 1

GTP, guanosine triphosphate

Hh, hedgehog

IQSec, IQ motif and Sec7 domain protein

IL, Interleukin

JIP, c-Jun-N-terminal-kinase interacting protein

JLS, jugular lymph sac

JV, jugular vein

LEC, lymphatic endothelial cell

LYVE-1, lymphatic vessel hyaluronan receptor-1

MHC, major histocompatibility complex

NDP, nucleoside diphosphate

NSF, *N*-ethylmaleimide-sensitive factor

PA, phosphatidic acid

PC, phosphatidylcholinePI4P, phosphatidylinositol 4-phosphate

PI(4,5)P$_2$, phosphatidylinositol 4,5-bisphosphate

PIP5K, phosphatidylinositol 4-phosphate 5-kinase

PLD, phospholipase D

Prox1, prospero-related homeobox gene 1

SAR, secretion associated and Ras-related protein

SMAP, stromal membrane-associated protein 1

SNAP, soluble NSF attachment protein

SNARE, SNAP receptor

Sox18, SRY-box 18

TfnR, transferrin receptor

TBC domain, Tre-2/Bub2/Cdc16 domain

VEC, vascular endothelial cell

VEGF-C, vascular endothelial growth factor-C

Nrp2, Neuropilin 2

Abstract

The small G protein ADP-ribosylation factor 6 (Arf6) plays pivotal roles in a wide variety of cellular events such as endocytosis, exocytosis, and actin cytoskeleton reorganization. However, the physiological functions of Arf6 at the whole animal level have not yet been thoroughly understood. The purpose of this study is to clarify physiological functions of Arf6 in lymphatic endothelium in mice. Here, I show that Arf6 regulates developmental and tumor lymphangiogenesis in mice. I generated and analyzed lymphatic endothelial cell (LEC)-specific *Arf6* conditional knockout (LEC-*Arf6* cKO) mice, and found that these mouse embryos exhibit severe skin edema and impairment in the formation of lymphatic vessel network at the mid-gestation stage. Furthermore, I found that knockdown of Arf6 in human LECs inhibits *in vitro* capillary tube formation and directed cell migration induced by vascular endothelial growth factor-C (VEGF-C), and Arf6 mediates VEGF-C-induced cell migration through the internalization of β1 integrin. Finally, it was found that LEC-*Arf6* cKO mice transplanted with B16 melanoma cells attenuated tumor lymphangiogenesis and progression. Collectively, these results provide evidence that Arf6 in LECs plays a crucial role in physiological and pathological lymphangiogenesis.

Contents

1. Introduction

1-1. Small GTPase

Small GTPases or small guanine nucleotide-binding proteins (small G proteins) with molecular weight of about 20 kDa are conserved from yeast to human [1]. To date, more than 100 membranes of small G protein superfamily have been identified, and are classified into five families including Ras, Rho, Rab, Ran, and Arf family based on similarity of their functions and sequences (Figure 1A). Small G proteins cycle between GDP-bound inactive and GTP-bound active forms to regulate a wide variety of cellular functions, such as gene expression, cytoskeletal reorganization, vesicle trafficking, nucleocytoplasmic transport, and microtubule organization (Figure 1B). In the resting state of the cell, they exist as the GDP-bound inactive form. Upon stimulation of the cell by
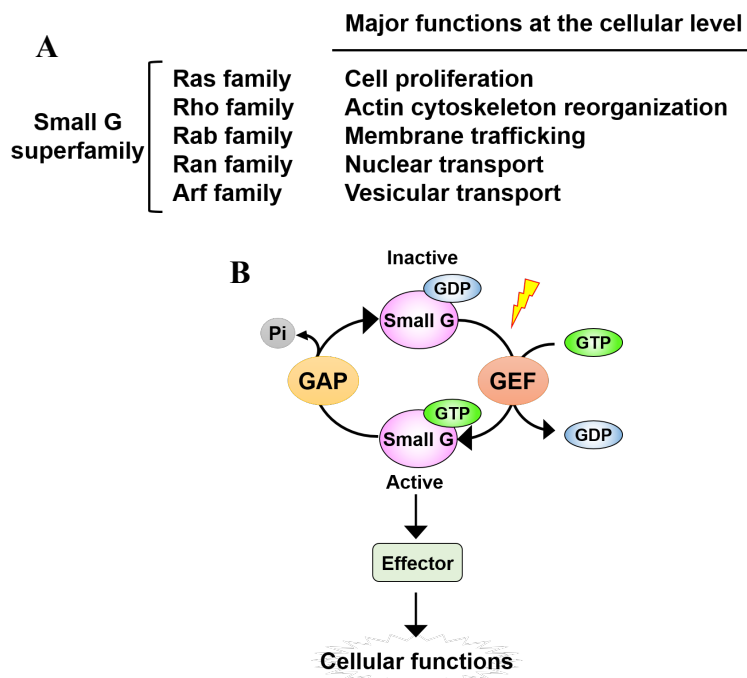
Figure 1. Small G protein superfamily

(**A**) Small G protein superfamily. Five families of small G protein including Ras, Rho, Rab, Ran, and Arf are categorized based on their functions. (**B**) Small G protein functions as molecular switches in signal transduction pathways by cycling between GDP-bound inactive and GTP-bound active states, which are precisely regulated by GEFs and GAPs. The activated small G protein transduces signals downstream. Thereafter, GTP on small G protein is hydrolyzed to GDP by the GTPase activity of small G protein, which is activated by GAPs, to become inactive.

2

agonists, such as hormones and growth factors, GDP on small G proteins is replaced for GTP to become active, which is accelerated by the guanine nucleotide exchange factors (GEFs). Activated small G protein interacts with their downstream effectors to transduce signals by regulating the cellular location and activity of effectors. Thereafter, GTP bound to small G proteins is hydrolyzed by their GTPase activity. Since the GTPase activities of small G proteins are very low, GTPase-activating proteins (GAPs) function to stimulate the GTPase activity of small G proteins. Thus, GEFs and GAPs support cycling of small G proteins between the inactive and active status for small G proteins to regulate signaling transduction and small G proteins function as molecular switches in signal transduction pathways.

1.2. Arf family

Arf proteins were first identified by Kahn, et al. as cofactors for cholera toxin-catalyzed ADP-ribosylation of α-subunit of the heterotrimeric GTP-binding protein Gs, which stimulates adenylyl cyclase [2]. At present, Arfs are known to regulate membrane traffic by recruiting coat proteins, phospholipid metabolism and reorganization of actin cytoskeleton [3, 4]. Arf family is composed of Arf proteins, structurally resemble Arf-like proteins (ARLs) and Arf-related proteins (ARPs), and the secretion-associated and Ras-related protein (SAR) [5]. The mammalian Arf proteins consist of Arf1-6, which are classified into three classes based on their sequence homology: Class I includes Arf1, Arf2, Arf3, class II Arf4 and Arf5, and class III (Arf6) (Figure 2) [4]. Class I and II of Arfs localize on the endoplasmic reticulum and Golgi apparatus. The sole member of class III, Arf6, localizes at the plasma membrane and endosomal compartments, such as early endosome and recycling endosome. These spatially specific locations of Arfs differentiate their functions in the cell. Class I and II of Arfs regulate the assembly of different types of coat protein complexes on budding vesicles along the secretory pathway [6] and recruitment of coat components to trans-Golgi membranes [7, 8]. On the other hand, Arf6 plays pivotal roles in endosomal membrane trafficking and actin cytoskeleton reorganization [4, 9, 10].

3
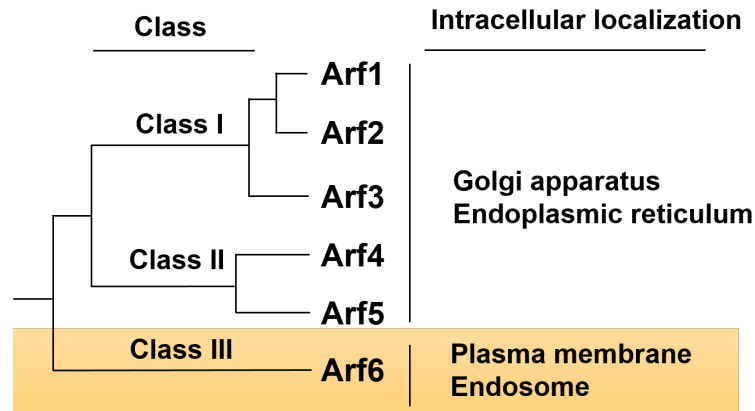
Figure 2. Mammalian Arf proteins and their cellular localization

Arf proteins are composed of 6 isoforms, Arf1-6, which are classified into 3 classes based on their sequence homology. Class I and II of Arfs localize to the Golgi apparatus and endoplasmic reticulum. Arf6, the sole member of class III, localizes at the plasma membrane and endosome.

The structure of Arf6 contains the N-terminal amphipathic helix, the effector-binding regions, switch1 (SW1) and SW2, and an interswitch region (Figure 3) [11]. Arf6 is post-translationally myristoylated at the N terminus, and this modification is essential for membrane binding and biological activity of Arf6 [11]. The myristoyl chain and associated N-terminal amphipathic helix are inserted into the membrane when Arf6 is activated [12]. SW1 and SW2 regions change their conformations in response to the Arf6 activation and are involved in interactions with Arf6 effectors [13]. Therefore, Arf6 effectors are expected to localize cellular components where the GTP-bound active form of Arf6 localizes.

Figure 3. Scheme of structure domains of Arf6

Arf6 contains an amphipathic helix at N-terminal, which is post-translationally myristoylated, two effector-binding regions of switch1 (SW1) and SW2, and an interswitch region between the two effector-binding regions.

4

1-3. Arf6 GEFs and GAPs

To date, 14 members of Arf GEFs family, which are classified into exchange factor for Arf6 (EFA6), cytohesin, brefeldin A-resistant Arf-guanine nucleotide exchange factor (BRAG), Golgi-specific brefeldin A-resistant Arf-guanine nucleotide exchange factor 1 (GBF1), and brefeldin A-inhibited GEF (BIG) subfamilies, have been identified (Figure 4) [14, 15]. Of these Arf GEFs, 8 members have been identified to be specific to Arf6. Their structures conserve the Sec7 domain, which is responsible for GEF activity to Arfs. The mammalian EFA6 family is composed of four proteins, EFA6A, EFA6B, EFA6C and EFA6D [16], which are highly selective for Arf6 [17]. Three BRAGs are BRAG1 (IQSec2), BRAG2 (IQSec1/GEP100) and BRAG3 (IQSec3/synArf6 GEF) [15], but only BRAG2 is specific for Arf6 [18]. Cytohesins are expressed in all vertebrates in four isoforms, cytohesin1, cytohesin2/ARNO, cytohesin3/Grp1 and cytohesin4 [15].

Arf GAP family so far identified includes 31 members, which are classified into ACAP, ARAP, ASAP, GIT, SMAP, ADAP, ArfGAP1, ArfGAP2, AGAP and AGFG subfamilies (Figure 4). They conserve the zinc-finger Arf GAP domain, which is responsible for stimulating GTPase activity of Arfs. Although the specificity of each member of Arf GAPs to Arf isoforms has not yet been fully clarified, *in vitro* analyses have revealed that at least 9 members of Arf GAPs are specific to Arf6.
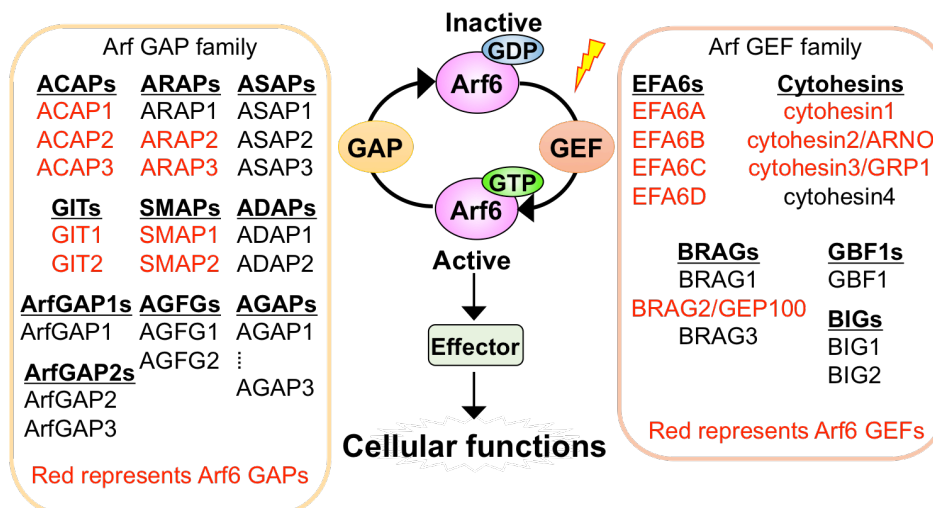
Figure 4. Arf6 GEF and GAP family members

To date, 8 members of Arf6 GEFs, which belong to BRAG, cytohesin, and EFA6 families, and 9 members of Arf6 GAPs, which belong to GIT, ARAP, ACAP, and

SMAP families, have been identified. They are shown in red color.

1.4. Arf6 effectors

Arf6 effectors so far identified, which are classified into three groups, phospholipid-metabolizing enzymes, Arf6 GAPs and others, are shown in Figure 5. The active form of Arf6 regulates a wide variety of cellular functions through the regulation of locations and activities of these effectors.
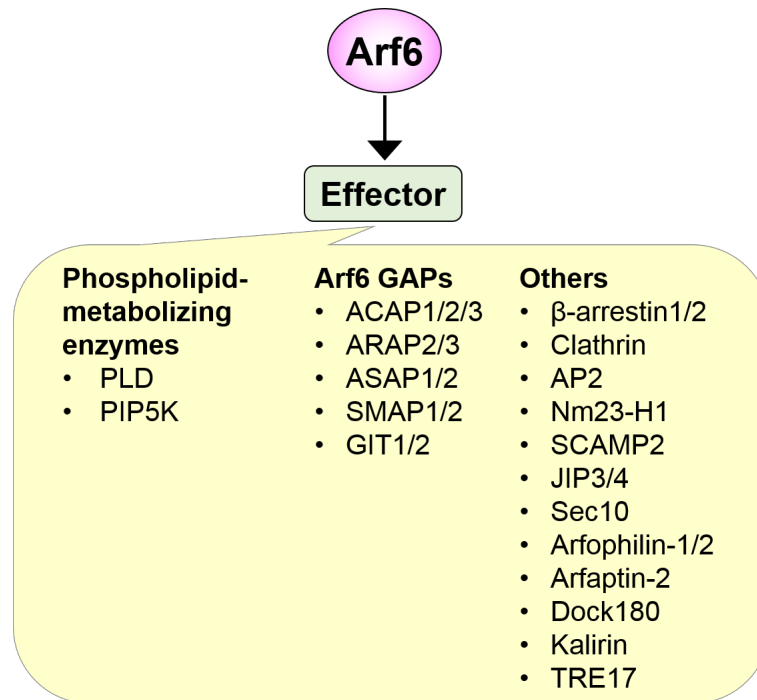
Figure 5. Effector proteins of Arf6

Three types of Arf6 effector proteins are described, including phospholipid-metabolizing enzymes, Arf6 GAPs, and others.

1-4-1. Phospholipid-metabolizing enzymes

Arf6 has been shown to activate two lipid-metabolizing enzymes, phospholipase D (PLD) (Figure 6) [19, 20] and phosphatidylinositol 4-phosphate 5-kinase (PIP5K) [21, 22]. PLD catalyzes the hydrolysis of phosphatidylcholine (PC) to the lipid messenger phosphatidic acid (PA), which controls membrane ruffling, endocytosis, exocytosis, stress fibers induction, respiratory burst, and Golgi transport (Figure 6) [23]. PIP5K generates the pleiotropic phospholipid phosphatidylinositol 4,5-bisphosphate [PI(4,5)P$_2$] by phosphorylating phosphatidylinositol 4-phosphate (PI4P) at the 5 position of the inositol ring: PI(4,5)P$_2$ regulates membrane channel activity [24], membrane trafficking [25], Golgi structure and

function [26, 27], actin dynamics [28], and nuclear activities (Figure 6) [29]. Interestingly, PA functions as a cofactor in the activation of PIP5K by Arf6, and PI(4,5)P$_2$ interacts with and activates PLD (Figure 6) [30]. This crosstalk explains these two Arf6 downstream effectors share the regulation of the same cellular functions. Thus, Arf6 mediates multiple cellular functions through regulating PLD and PIP5K activities.
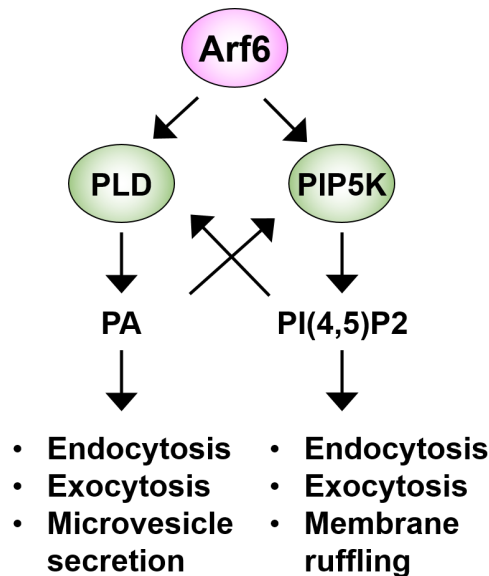
Figure 6. Arf6 activates PLD and PIP5K to regulate a wide variety of cellular functions

Arf6 activates PLD and PIP5K to produce PA and PI(4,5)P$_2$, respectively, to regulates cellular functions described in the figure. PA and PI(4,5)P$_2$ support the activation of PIP5K and PLD by Arf6, respectively.

1-4-2. Arf6 GAPs

Arf6 GAPs are listed in Figures 4 and 5. In addition to the function of Arf6 GAPs to support the hydrolysis of GDP on Arf6 by stimulating the GTPase activity of Arf6, Arf6 GAPs seem to function as a recruiter of signaling molecules (Figure 7) [31-34]. For instance, ACAP1 is involved in β1 integrin recycling by associating endosomal β1 integrin [35]. Moreover, SMAP1 has been reported to participate in the clathrin-dependent and constitutive endocytosis of transferrin receptor (TfnR) [31]: Arf6-bound SMAP1 recruits clathrin and the adaptor protein complex-2 (AP-2) to the plasma membrane, thereby stimulating endocytosis of TfnR. Additionally, ASAP1 interacts with cortactin and paxillin to form a trimeric protein complex, which is critical for the formation of invadopodia [36]. In this sense, Arf6 GAPs

function as effector proteins of Arf6 in a wide variety of signaling pathways.
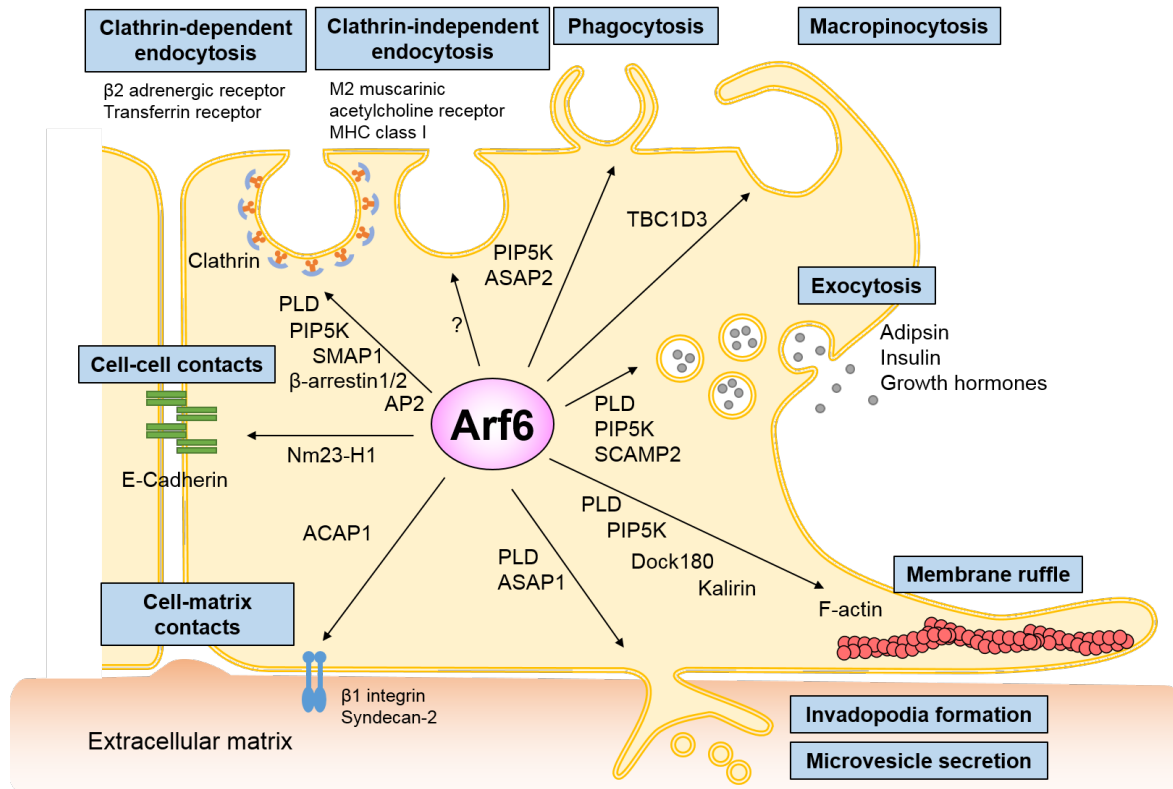
Figure 7. Arf6 effectors including Arf6 GAPs and other signaling molecules
Arf6 regulates cellular functions through a wide variety of effectors, such as Arf6 GAPs, lipid-metabolizing enzymes, and other effectors, to regulate membrane traffic of receptors, cadherins, and integrins. The cellular signaling through these effectors control cell motility, and membrane ruffle formation by reorganization of the actin cytoskeleton.

1-4-3. Other Arf6 effector proteins

In addition to the phospholipid-metabolizing enzymes and GAPs, other proteins also function as downstream effectors for Arf6 to regulate cellular functions (Figure 7). For example, monomeric clathrin adaptors β-arrestin1/2 that bind clathrin and PI(4,5)P$_2$ to recruit cargo and promote clathrin-dependent endocytosis functions as an Arf6 effector [37]. The nucleoside diphosphate (NDP) kinase Nm23-H1 is recruited to the cell-cell contact region and provides a source of GTP during dynamin-dependent vesicle fission in an Arf6-dependent manner [38, 39]. The secretory carrier membrane protein, SCAMP2, functions in setting up the soluble NSF attachment protein (SNAP) receptor (SNARE) interactions with the secretory vesicle

and plasma membranes, and facilitates fusion pore formation in the SNARE-mediated fusion of the vesicle exocytosis [40]. The c-Jun-N-terminal-kinase interacting protein 3 (JIP3) and JIP4 interact with kinesin-1 and dynactin complex to control the trafficking of recycling endosomes during cytokinesis in an Arf6-dependent manner [41]. Sec10, the subunit of the exocyst complex, is involved in docking of vesicles with the plasma membrane and regulates the post-endocytic recycling downstream of Arf6 [42, 43]. The dual Rab11/Arf6 binding proteins, FIP3/Arfophilin-1 and FIP4/Arfophilin-2, regulates cytokinesis through coupling with Rab11-positive vesicle traffic from recycling endosomes to the cleavage furrow [44]. Arfaptin-2, to which Arf6 binds to, is known as the partner of Rac1 and regulates cytoskeletal rearrangements at the cell periphery [45]. The Rac1 GEF Dock180 and Kalirin were both indicated to mediate cytoskeletal and focal adhesion regulation through control the activity of Rac1 downstream of Arf6 [46]. Tre-2/Bub2/Cdc16 (TBC) domain-containing protein TRE17 regulates plasma membrane-endosome trafficking via promoting the localization of Arf6 to the plasma membrane and Arf6 activation [47]. Thus, these molecules are believed to be Arf6 effectors.

1-5. Cellular functions of Arf6

1-5-1. Endocytosis

Arf6 mediates clathrin-dependent endocytosis of membrane proteins, such as TfnR [9], β2-adrenergic receptor [48], E-cadherin [49] and G-protein-coupled receptors (GPCRs) (Figure 7) [50]. The initial step of endocytosis of cell membrane proteins is the translocation of the active form of Arf6 from the cytosol to the plasma membrane. In the clathrin-mediated endocytosis, the active form of Arf6 binds to and activates PIP5K to produce $PI(4,5)P_2$ [21], which regulates clathrin-mediated endocytosis [51] via the recruitment of AP-2 and clathrin on coated pits formed at the plasma membrane [22, 52]. Thereafter, Arf6 GAPs trigger the budding of vesicles from the plasma membrane by inactivating Arf6 [31]. Interestingly, vesicle formation and budding from the plasma membrane are determined by a cargo protein. For example, the Arf6 GAP SMAP1 functions in the endocytosis of TfnR [53]. GIT1 plays a role in the interleukin (IL)-mediated endocytosis of GPCRs and epidermal growth factor receptors (EGFRs) [50]. Thus, the GTP/GDP cycling of Arf6 coordinates the recruitment of AP-2 and clathrin to activated receptors during the endocytic process [54].

Arf6 also regulates the clathrin-independent endocytosis (CIE) pathway (Figure 7). The

cargo proteins include the major histocompatibility complex class I protein (MHC class I), M2-muscarinic acetylcholine receptors, and the peripheral myelin-membrane protein [4]. Cargos through Arf6-associated CIE are sorted to recycling or degradation pathway based on specific cytoplasmic sequences [55, 56] and ubiquitination of the cytoplasmic tails of these cargo proteins [57]. However, the detailed mechanism of the CIE pathway is still unclear and requires more investigation.

1-5-2. Cell adhesion

In epithelial cells, Arf6 modulates the cell-cell contact through recruiting Nm23-H1 for facilitating dynamin-dependent endocytosis of E-cadherin (Figure 7) [39]. This endocytosis of E-cadherin leads the disassembly of adherens junctions, thereby regulating epithelial cell scattering and the epithelial-mesenchymal transition (EMT) of cancer cells. Arf6 also regulates the contact of cell-extracellular matrix (ECM) via trafficking of β1 integrin and syndecan-2 (Figure 7) [58-60].

1-5-3. Invadopodia formation and microvesicle releasing

It has been reported that Arf6 is involved in cancer invasion and GTP/GDP cycle of Arf6 is critical for the invasion of melanoma, glioma, and breast cancer cells (Figure 7) [4, 55, 61-63]. Moreover, Arf6 has been implicated in the regulation of invadopodia formation/turnover [4] and protease secretion to degrade ECM [62]. Invadopodia are actin-rich membrane protrusions with integrins and associated signaling proteins. In order to form the invadopodia, Arf6 recruits the Arf6 GAP ASAP1 to link paxillin and cortactin in malignant breast cancer cells [34]. For the protease release from tumor cells to degrade ECM, Arf6 modulates the shedding of plasma membrane-derived microvesicles with protease cargo into the surrounding environment through phospholipid metabolism and the activation of extracellular signal-regulated kinase (ERK) [62].

1-5-4. Exocytosis

Arf6 has been implicated in the regulation of protein secretion (Figure 7). For instance, the secretion of adipsin from adipocytes [64], neurotransmitters and human growth hormones by Ca^{2+}-dependent dense-core vesicle (DCV) exocytosis from PC12 cells [65, 66], and insulin from pancreatic β cells [67]. SCAMP2 interacts with PLD1, Arf6, and ARNO, and this association is crucial for the SNARE-mediated fusion of vesicles with the plasma membrane

for exocytosis [40]. Arf6-mediated exocytic pathway also requires activation of PIP5K by Arf6 to increase $PI(4,5)P_2$ level on the plasma membrane [67].

1-5-5. Membrane ruffle formation

Membrane ruffle formation requires activation of peripheral PIP5K through Arf6 to produce $PI(4,5)P_2$ (Figure 7) [21], which induces reorganization of actin cytoskeleton. In addition, Arf6 effectors, the Rac1 GEF Dock180 and Kalirin, activate Rac1 [68, 69], leading to the rearrangement of actin cytoskeleton in the signaling pathway for membrane ruffle formation.

1-5-6. Phagocytosis

During phagocytosis, membranes are delivered from internal stores to particle internalization sites of the plasma membrane to accommodate pseudopod extension and ingest particles. Arf6 is involved in Fc receptor (FcR)-regulated phagocytosis, which is thought to require actin cytoskeleton reorganization (Figure 7) [70-73] and occur through the activation of the Rac1 and lipid metabolism [74].

1-5-7. Macropinocytosis

Macropinocytosis is the process to engulf the large volumes of fluid by extension, folding and closure of the plasma membranes [75]. To drive internalization, the actin filaments generate forces by modulating dynamics of actin assembly [76, 77], which form the dorsal ruffles. It has been shown that the Arf6 effector domain-containing proteins regulate membrane trafficking (Figure 7) [78]. The primate-specific TBC1D3 regulates EGF-mediated macropinocytosis in an Arf6-dependent manner [79]. In addition, TBC1D3 interacts and coordinates with Golgi-localized, gamma adaptin ear-containing, Arf-binding protein 3 (GGA3) to facilitate the macropinocytotic process. Interestingly, TBC1D3 lacks the arginine residue that is responsible for the Rab-GAP activity, but there is no clear evidence of its Arf6-GAP activity. Interestingly, another TBC protein TRE17 has been shown to bind to the GDP-form of Arf6 and activate Arf6 for regulation of the plasma membrane-endosome trafficking via cooperating with Arf6 GEFs [47].

1-5-8. Proliferation

Arf6 has been indicated to regulate cell proliferation and mitosis (Figure 7) [80-82]. Arf6 induces cell proliferation through activating PLD and S6K1 kinase in a

PLD-mTORC1-dependent manner, thereby contributing to mitosis [83]. In addition, P38 MAPK accelerates the Arf6-mediated cell proliferation. It has been revealed that EGF-induced Arf6 expression plays an important role in the proliferation of glioma cells [84]. Arf6 also regulates hedgehog (Hh) signaling through cooperating with EGFR to induce Ras tumor growth [85]. Arf6 activates TRE17 to promote cell proliferation [86]. Arf6 activation induces the trafficking of β-catenin and guanine nucleotide-binding protein G(q) subunit α (GNAQ) from the plasma membrane to the nucleus and cytoplasmic vesicles, receptively [87]. Thereafter, multiple signaling pathways through Rho/Rac, YAP, and PLC/PKC are activated, which are involved in the proliferation of melanoma cells.

1-6. Physiological functions of Arf6

Although the functions of Arf6 at the cellular level have been well studied, the physiological significance of Arf6 remain unclear. To address this issue, the laboratory to which I belong had generated *Arf6* knockout (*Arf6^-/-*) mice, and analyzed them. Kanaho and his colleagues have reported that *Arf6^-/-* mice are embryonic lethal at midgestation with defect in the liver development [88]. Moreover, they have generated several tissue- and cell type-specific conditional knockout (cKO) mice, and found that endothelial-specific *Arf6* cKO mice show the defect in tumor angiogenesis [60] and that keratinocyte-specific *Arf6* cKO mice show a significant delay in the wound healing of the skin [89]. Neuron-specific *Arf6* cKO mice display the defect in the oligodendrocyte myelination in the hippocampal fimbria and the corpus callosum [90]. Platelet-specific *Arf6* cKO mice show the defect in platelet spreading and blood clot by causing the aberrant αIIbβ3 integrin trafficking [91].

1-7. Lymphangiogenesis

The lymphatic system is comprised of a blind-ended network of lymphatic vessels, which collect and transport the interstitial fluid and lymph, and plays critical roles in homeostasis of tissue fluid, lipid absorption, and immune surveillance. Malfunction of lymphatic vessels is pivotal and associate with a wide variety of diseases such as inflammation, fibrosis, metastasis, and lymphedema [92]. Development of lymphatic vasculature in the embryo initiates from a subset of venous endothelial cells that follow by the specification of lymphatic endothelial cell fate, sprouting, morphogenesis, and network formation (Figure 8). Venous endothelial cells expressing the lymphatic vessel hyaluronan receptor-1 (LYVE-1) in the central veins serve as lymphatic endothelial cell (LEC) precursors, which express the

transcription factor SRY-box 18 (Sox18) to express the key transcription factor prospero-related homeobox gene 1 (Prox1), the marker for LECs, in mice at approximately embryonic day (E) 9.5 [93]. Prox1-expressing LECs in the cardinal vein assemble the pre-lymphatic clusters, migrate away from the cardinal vein wall to form the lymph sacs and superficial lymphatic vessels at E10.5-13.5 [93-96]. The sprouting of lymphatic vessels from the lymph sac is induced by VEGF-C through its receptor VEGFR3 [97], which regulates receptor modulators such as Neuropilin 2 (Nrp2) [98], Ephrin B2 [99] and β1 integrin [100-102] to generate the lymphatic vascular network in mouse embryos within E14.5. In addition, LECs express the membrane glycoprotein podoplanin [103, 104], which activates the Syk tyrosine kinase through C-type lectin receptor 2 (CLEC-2) in platelets [105, 106]. This activation leads to platelet aggregation [106, 107]. From E15.5 to postnatal stage, the primary lymphatic networks undergo remodeling to form a mature lymphatic network composed of initial lymphatic vessels, pre-collectors and collecting lymphatic vessels [108]. Finally, these lymphatic network forms intraluminal valves, recruits smooth muscle cells, develop continuous inter-endothelial junctions, and produce a basement membrane [92].
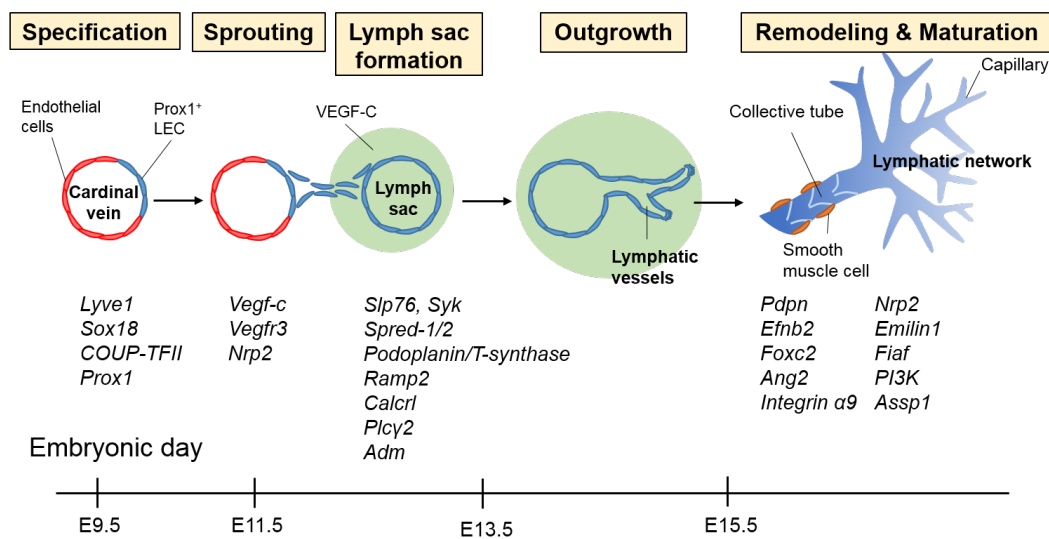
Figure 8. Lymphangiogenesis during mouse embryonic development

During embryonic lymphatic vessel development, a subset of LECs in cardinal vein expresse Prox1, and migrate out to form the lymph sac. Thereafter, lymphatic vessels are formed and then initiate outgrowth in response to VEGF-C to construct the lymphatic network. Various markers are identified and specifically expressed in developing cells.

13

1-8. Tumor lymphangiogenesis

It has been known that cancer cells disseminate or metastasize to distal organs via either angiogenesis or lymphangiogenesis (Figure 9). Since the lymphatic vessels are single thin layers and have larger diameters than blood vessels [92], cancer cells easily invade into the lymphatic system. More evidence revealed that the density of lymphatic vessels correlates with the incidence of lymph node metastasis and poor prognosis in some human cancers [109, 110], indicating that tumor lymphangiogenesis is a pivotal process for cancer progression and metastasis. Tumor lymphangiogenesis is mediated by lymphangiogenic factors, VEGF-C and VEGF-D, that are produced by tumors, stromal cells, macrophages, and activated platelets [111-114]. These factors stimulate growth and dilation of the peritumoral lymphatic vessels, thereby enhancing tumor cell invasion into lymphatic vessels and lymph node, and facilitating dissemination of tumor cells to distal organs [109, 115-117]. Therefore, blockage of lymphangiogenic factors has been implied in the suppression of metastasis: blockage of VEGFR3 signaling in mice significantly reduces tumor lymphangiogenesis and lymphatic metastasis [118-121]. Inhibition of neuropilin-2 inhibits lymphatic endothelial cell migration, resulting in the suppression of tumor lymphangiogenesis and metastasis to sentinel lymph nodes [122].
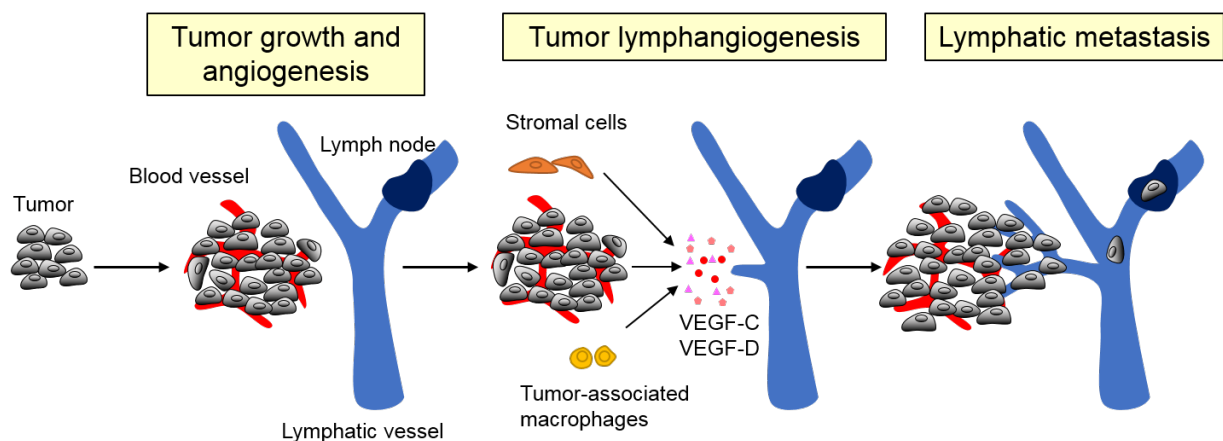
Figure 9. Tumor lymphangiogenesis

In tumor environment, not only tumor cells but also inflammatory cells and stromal cells secret various lymphatic growth factors. These factors stimulate tumor lymphangiogenesis, which facilitates the invasion of cancer cells into the lymphatic system.

14

1-9. Lymphatic disorder

Several lymphatic genes have been identified by lineage-tracing studies in mice to validate the development of lymphatic vessel and association with human lymphatic disorders. For example, the VEGFR3 mutation causes Milroy disease [123], and mutation in its ligand VEGF-C is associated with autosomal dominant Milroy-like lymphedema [124]. Hypotrichosis-lymphedema-telangiectasia patients have a mutation in transcription factor *SOX18*, which has been identified to induce Prox1 expression in venous LEC progenitors [125, 126]. *Collagen and calcium binding EGF domains 1 (CCBE1)* mutations cause lymph vessel dysplasia that associate with Hennekam syndrome [127, 128]. Mutation of *Forkhead box protein C2 (FOXC2)*, which regulates lymphatic valves formation and lymphatic remodeling, was found in lymphedema-distichiasis syndrome [129].

Although various guidance molecules, cellular interactions, and extrinsic forces are involved in embryonic lymphangiogenesis [130], the molecular mechanisms for lymphatic vascular network formation are poorly understood and require more research to elucidate it.

2. Aim

Since the small G protein Arf6 plays pivotal roles in a wide variety of cellular events, such as endocytosis, exocytosis, and actin cytoskeleton reorganization [14, 21], the physiological functions of Arf6 at the whole animal level have not been well elucidated. In the previous study, it has been demonstrated that $Arf6^{-/-}$ mice are embryonic lethal at midgestation with liver development defect [88]. Here, I aim to re-examine the different stages of $Arf6^{-/-}$ embryos in depth and clarify the cause of edema in $Arf6^{-/-}$ embryos. In addition, I aim to elucidate the physiological and pathological functions of Arf6 in LECs by generating LEC-specific Arf6 cKO mice and analyzing them.

3. Materials and methods

Mice

Arf6⁻/⁻ and *Arf6^{flox/flox}* mice were generated as described previously [60, 88, 90]. LEC-*Arf6* cKO mice were generated by mating *Arf6^{flox/flox}* and *Prox1-CreER^{T2}* mice, which were kindly provided by Dr. S. Ito (Showa Pharmaceutical University, Japan) [94]. To initiate Cre-mediated recombination in embryos, pregnant mice were intraperitoneally injected with 3 mg of tamoxifen dissolved in sunflower oil every day from E10.5 [94]. *ROSA26-CAGp-loxP-EGFP-loxP-tdsRed* (*R26GRR*) mice provided by Dr. S. Takahashi (University of Tsukuba, Japan) were used to validate the Cre activity in LECs [131, 132]. All experiments using mice were performed according to the Guidelines for Proper Conduct of Animal Experiments, Science Council of Japan, and the protocols were approved by the Animal Care and Use Committee of University of Tsukuba.

Whole-mount immunofluorescence staining of embryonic dorsal skin

After mouse embryos were fixed with 4% paraformaldehyde (PFA)/PBS at 4°C and subsequently dehydrated in methanol, the dorsal skin was dissected, rehydrated in PBST (0.2% Tween-20/PBS), and incubated in the blocking buffer consisting of 0.1 M Tris-HCl, pH7.5, 0.5% blocking reagent (PerkinElmer Life Sciences) and 0.15 M NaCl for 1 hr at room temperature (r.t.). The skin samples were incubated with the primary antibodies against LYVE-1 (Abcam), Prox1 (R&D Systems), PECAM-1 (BD Biosciences), or Ki67 (Abcam) at 4°C overnight and subsequently with Alexa Fluor®-488-, Alexa Fluor®-546-, Alexa Fluor®-594-, Cy3-, and Cy5-conjugated secondary antibodies (Thermo Fisher Scientific). Immunofluorescence images were obtained with Biozero BZ-X700 microscope (Keyence, Japan) or Leica TCS SP5 confocal microscope. The branch number, total vessel length, and width of lymphatic vessels were analyzed by NIH ImageJ software.

Tissue sections and immunohistochemical analysis

Embryos were fixed with 4% PFA/PBS at 4°C overnight, equilibrated in 30% sucrose/PBS, then embedded in OCT compound. Embedded embryos were cryosectioned at 14-16 μm, and subjected to immunohistochemical analysis. For the immunohistochemical analysis, sections were washed with PBS, and blocked with the blocking buffer at r.t. for 1 hr. Sections were then incubated with anti-Arf6, which was kindly provided by Dr. H. Sakagami (Kitasato University, Japan), anti-LYVE-1, anti-Prox1, or anti-PECAM-1 antibody at 4°C overnight.

After washing with PBST, sections were incubated with Alexa Fluor®-488 goat anti-rabbit IgG antibody at r.t. for 1 hr, and counterstained with DAPI. Images were obtained with Biozero BZ-X700 microscope.

Isolation of primary mLECs and mVECs

Skins dissected from E16.5 embryos were digested with the solution consisting or 1 mg/ml of deoxyribonuclease I, 2.5 mg/ml of collagenase type II and type IV, 20% FBS, and 10 mM HEPES buffer in DMEM. Macrophages and hematopoietic cells were removed by incubating the cell suspension with rat anti-F4/80 (MCA497GA, Bio-Rad) and -CD45 antibody (B122583, BioLegend) and subsequently precipitating with goat anti-rat IgG microbeads (Miltenyi Biotec). Mouse LECs (mLECs) and mouse VECs (mVECs) in the cell suspension were captured by rabbit anti-LYVE-1 (ab14917, Abcam,) and rat anti-PECAM-1 antibody (102501, BioLegend), and precipitated with goat anti-rabbit IgG microbeads (Miltenyi Biotec). Captured mLECs and mVECs were sorted using The MiniMACS™ kit (Miltenyi Biotec) as described previously.[133] Isolated mLECs and mVECs were immediately used for detection of mRNAs and proteins.

Reverse transcription and quantitative real-time PCR

Total cellular RNA was extracted from the cells using the TRIzol® Reagent (Life Technologies, Carlsbad, CA). The reverse transcription of the RNA (1.5 μg) was performed in a 30 μl reaction mixture using SuperScriptTM III Reverse Transcriptase (Thermo Fisher Scientific) and oligo-dT primers. Quantitative real-time PCR (qRT-PCR) reactions were conducted in Applied Biosystems 7500/7500 Fast Real-Time PCR System (Thermo Fisher Scientific) using THUNDERBIRD™ SYBR® qPCR Mix (TOYOBO) according to manufactory's instruction. The thermal profile of PCR was at 95°C for 3 min, followed by 40 cycles at 95°C for 30 sec and 60°C for 30 sec. The sequences of paired primers for qRT-PCR are as follows:

Actin beta (Actb) forward: 5'-GATCATTGCTCCTCCTGAGC-3'
Actb reverse: 5'-GTCATAGTCCGCCTAGAAGCAT-3'
Prox1 forward: 5'-CTGGGCCAATTATCACCAGT-3'
Prox1 reverse: 5'-GCCATCTTCAAAAGCTCGTC-3'
Lyve1 forward: 5'-TGGTGTTACTCCTCGCCTCT-3'

Lyve1 reverse: 5'-TTCTGCGCTGACTCTACCTG-3'

Flt1 forward: 5'-AGCACCTTGACCTTGGACAC-3'

Flt1 reverse: 5'-CAGGGGATGATGAGCTGTCT-3'

Arf6 forward: 5'-TGCCTAAACTGGAGGAAACTTGAA-3'

Arf6 reverse: 5'-ACCACATCTCACCTGCAACATT-3'

GAPDH forward: 5'-AAGGTGAAGGTCGGAGTC-3'

GAPDH reverse: 5'-TGTAGTTGAGGTCAATGAAGG-3'

Cell culture and siRNA transfection

Human LECs (hLECs; Lonza) were cultured in EGM™-2 MV Medium (Lonza) and maintained within 5 passages. siRNAs for Arf6 (Dharmacon) were transfected with Lipofectamine 2000 (Thermo Fisher Scientific) according to the manufacturer's instruction. B16 melanoma cells were maintained in Dulbecco's modified Eagle medium (DMEM; Nacalai Tesque, Japan) supplemented with 10% fetal bovine serum, penicillin, and streptomycin.

Cell proliferation assay

For the cell proliferation assay, siRNA-transfected hLECs were cultured in EGM™-2 MV Medium on 35-mm dishes for two days and harvested by Accutase treatment (Nacalai Tesque), and the cell number was counted.

In vitro capillary tube formation by hLECs

hLECs cultured on 24-well plates coated with the growth factor-reduced Matrigel (BD Biosciences) at 1.5×10^5 cells per well were starved, transfected with siRNAs for Arf6, and stimulated with 200 ng/ml of VEGF-C (R&D Systems). After 12 hr of the stimulation, cell images were obtained using the Biozero BZ-X700 microscope, and the capillary tube length was measured by NIH ImageJ software.

Assays for wound healing and cell migration

For the wound healing assay, hLECs transfected with siRNA for Arf6 were grown on 24-well plates to full confluency and starved in serum-free EBM™-2 Basal Medium (Lonza) overnight. Monolayers of the cells were scratched with pipette tips and stimulated with 200 ng/ml of VEGF-C. Cell images were obtained with the Biozero BZ-X700 microscope, and

wound closure was analyzed by NIH ImageJ software.

For the transwell migration assay, hLECs starved as described above were seeded in the upper chamber of transwell migration chamber (8 μm pore size; Corning) at 2×10^4 cells per chamber. The lower chamber was filled with 200 ng/ml of VEGF-C/EBM^{TM}-2 Basal Medium. At 12 hr after seeding, membrane filters were fixed with 4% PFA/PBS and stained with DAPI. hLECs migrated to the lower surface of the membrane filter were imaged using the Biozero BZ-X700 microscope, and the cell number was counted.

For time-lapse analysis of wound-induced cell migration, hLECs transfected with siRNA for Arf6 were cultured on the μ-Dish dish (ibidi, Germany) to full confluency, and starved in serum-free EBM^{TM}-2 Basal Medium overnight. The monolayer of the hLECs was scratched with pipette tips, and then incubated in the humidified chamber of a time-lapse microscopy (FLUOVIEW FV10i, Olympus) in the presence or absence of 200 ng/ml of VEGF-C at 5% CO_2 and 37°C. Cell migration at the wounded area was recorded every 10 min for 20 hr by tracking the nucleus using the manual-tracking tool of NIH ImageJ. Cell trajectories were analyzed using the Chemotaxis and Migration Tool Software (ibidi). Accumulated distance was calculated as the sum of all cell movement. Euclidean distance represents the straight distance between the start and end point of cell migration. Directionality was calculated by dividing euclidean distance by accumulated distance.

Western Blotting

Western blotting was carried out as previously reported [60], using anti-Arf6 that was previously generated by us [134], anti-β1 integrin TS2/16 (Santa Cruz) and anti-α-tubulin (Sigma-Aldrich) antibodies.

Assay for the activated β1 integrin level and focal adhesion formation

To evaluate the activated β1 integrin levels at the plasma membrane, control and Arf6-knocked-down hLECs were stimulated with VEGF-C. Cells were fixed with 4% PFA/PBS, blocked with the blocking buffer, then immunostained by sequential incubation with anti-active β1 integrin (9EG7, BD Biosciences) and Alexa Fluor$^®$-488-conjugated secondary antibodies (Thermo Fisher Scientific). Immunofluorescence images were obtained with Biozero BZ-X700 microscope, and the fluorescence intensities for the activated β1 integrin were analyzed by NIH ImageJ software.

For focal adhesion formation assay, control and Arf6-knocked-down hLECs were

stimulated with VEGF-C for the indicated times. Cells were fixed, blocked, and stained with anti-paxillin (BD Biosciences) and Alexa Fluor®-488-conjugated secondary antibodies. Images were obtained by Leica TCS SP5 confocal microscope, and the focal adhesion formation was analyzed by ImageJ software.

Internalization of β1 integrin

Control and Arf6-knocked-down hLECs were incubated with anti-β1 integrin TS2/16 antibody for 30 min on ice. The β1 integrin/antibody complex on the plasma membrane was allowed to be internalized by incubating with 200 ng/ml of VEGF-C at 37°C for the indicated time in the presence of 0.6 μM of primaquine, an inhibitor for the recycling of β1 integrin to the plasma membrane. Anti-β1 integrin antibody on the cell surface was removed by washing with the ice-cold stripping solution (0.5% acetic acid, 0.5 M NaCl and 0.05% BSA). The cells were fixed with 4% PFA/PBS, permeabilized with 0.1% Triton X-100/PBS, and visualized for the internalized β1 integrin with Fluor®-488-labeled secondary antibody. Z-stack fluorescence images were obtained with Leica TCS SP5 confocal microscope, and the fluorescence intensities of internalized β1 integrin were analyzed by NIH ImageJ software.

Tumor lymphangiogenesis and tumor progression

LEC-*Arf6* cKO mice were administered with 3 mg of tamoxifen into peritoneal cavity once a day for 7 days and subcutaneously transplanted with B16 melanoma cells (2×10^6 cells) suspended in 100 μl of serum-free DMEM into the dorsal flank. From day 6 after the transplantation, tumor volumes were measured by digital caliper and calculated using the following formula: tumor volume = length × width^2 × 0.52. After 14 days of the transplantation, tumors were dissected, fixed with 4% PFA/PBS and subjected to assay for tumor lymphangiogenesis.

Statistical analysis

Student's *t*-test and ANOVA were used to calculate the statistical significance between two experimental groups and more than two experimental groups, respectively. The value of $P < 0.05$ was considered as statistical significance. Each result was obtained from at least three independent experiments, and all quantitated data are represented as mean ± SEM.

4. Results

Ablation of Arf6 from lymphatic endothelial cells causes edema and defect in lymphatic vascular network formation

As we have previously reported [60], the re-examination of $Arf6^{-/-}$ embryos confirmed that knockout of $Arf6$ induces the dorsal skin edema in E13.5 and E15.5 embryos (Figure 10A). Because impairment in lymphatic vascular formation causes hydrops fetalis with back skin edema [126, 135-137], we examined the lymphatic vascular network formation in the back skin of $Arf6^{-/-}$ embryos by immunofluorescent staining for the specific marker of mouse LECs (mLECs) LYVE-1 (Figure 10B). As expected, $Arf6^{-/-}$ embryos showed the aberrant morphology of the lymphatic vascular network: extension of the front tip of lymphatic vessels toward the dorsal midline was delayed in $Arf6^{-/-}$ embryos. Detailed analysis revealed the fewer branch points, shorter total vessel length, and enlarged lymphatic vessels in $Arf6^{-/-}$ embryos (Figure 10C). In support of these observations, embryonic Prox1^{+} and LYVE-1^{+} mLECs isolated from dorsal skins of E16.5 embryos (Figure 11A) expressed the Arf6 protein and its mRNA (Figure 11B,C). In addition, Arf6 was expressed in the lymph sac of E13.5 embryos (Figure 11D).
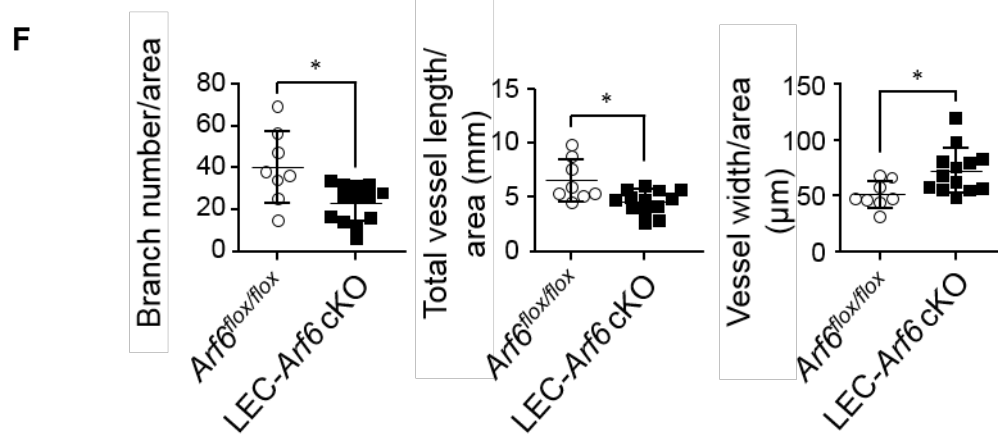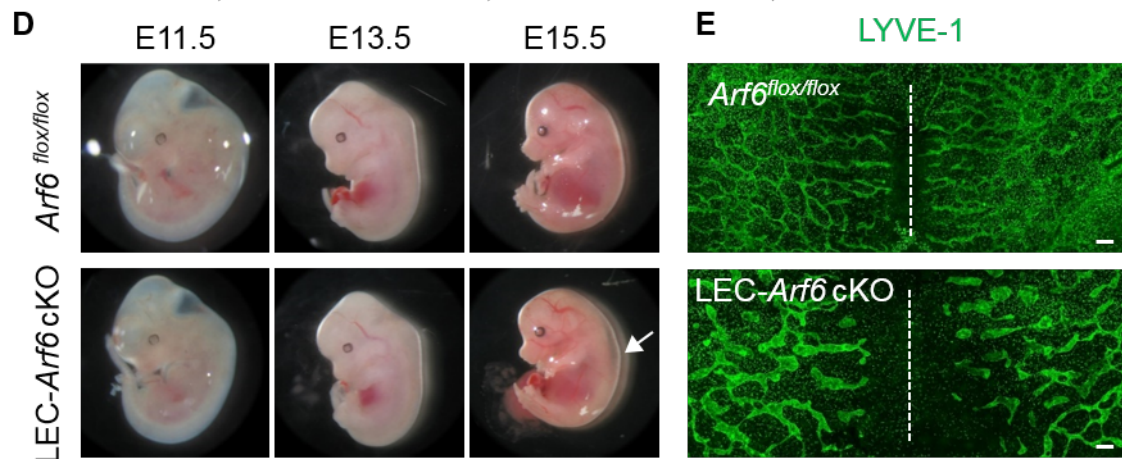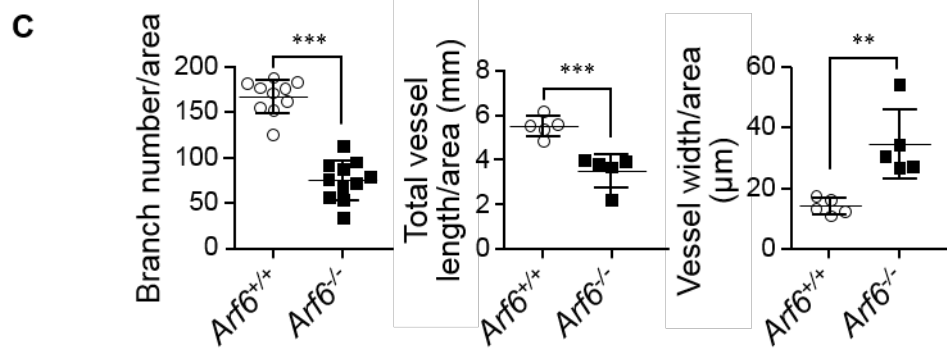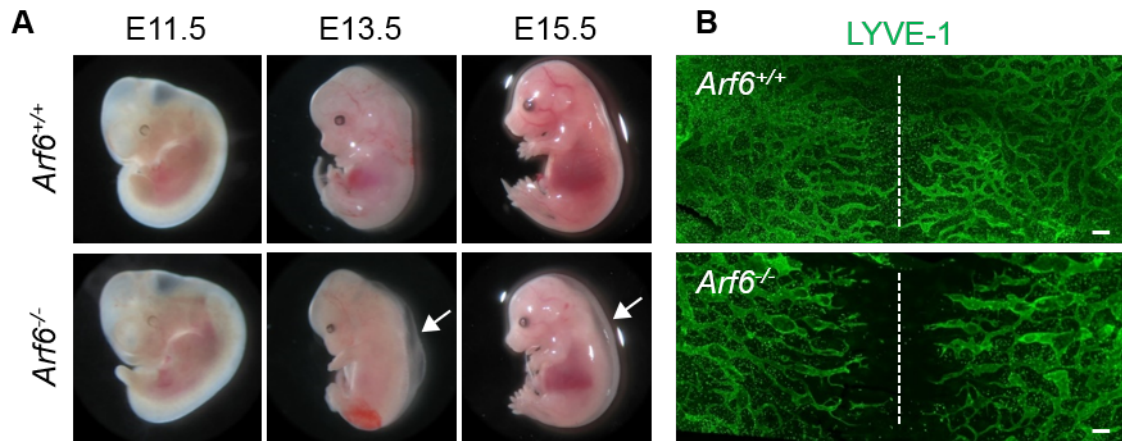
Figure 10. *Arf6* *Arf6*$^{-/-}$ and LEC-*Arf6* cKO mice induce dorsal skin edema and abnormal lymphatic vascular network

(A, D) Appearance of *Arf6*$^{-/-}$ and LEC-*Arf6* cKO embryos in comparison with that of control *Arf6*$^{+/+}$ and *Arf6*$^{flox/flox}$ embryos, respectively. Note that the edema (white arrows) on the back of E13.5 and 15.5 *Arf6*$^{-/-}$ embryos and of E15.5 LEC-*Arf6* cKO were induced. (B, E) Aberration of dorsal subcutaneous lymphatic vascular network in E15.5 *Arf6*$^{-/-}$ and LEC-*Arf6* cKO embryos. Lymphatic vessels were immunostained for LYVE-1 (green). White dashed lines indicate the dorsal midline of the embryo. (C, F) Immunostained images of lymphatic vessels shown in (A) were quantified for branch number of lymphatic vessels/area (left panel), lymphatic vessel length/area (middle panel), and width of lymphatic vessels/area (right panel) in control *Arf6*$^{+/+}$ and *Arf6*$^{-/-}$ embryos (C) and control *Arf6*$^{flox/flox}$ and LEC-*Arf6* cKO embryos (F). Area of 2250 × 1700 μm on both sides of the midline was measured. Each point represents individual value: n = 10 for both embryos in the left panel and n = 5 for both embryos in the middle and right panels of (C), and n = 8 for *Arf6*$^{flox/flox}$ embryos and n = 13 for LEC-*Arf6* cKO embryos in (F). Statistical significance was assessed using student's *t*-test. *$P < 0.05$, **$P < 0.01$, ***$P < 0.005$. Scale bar, 200 μm.
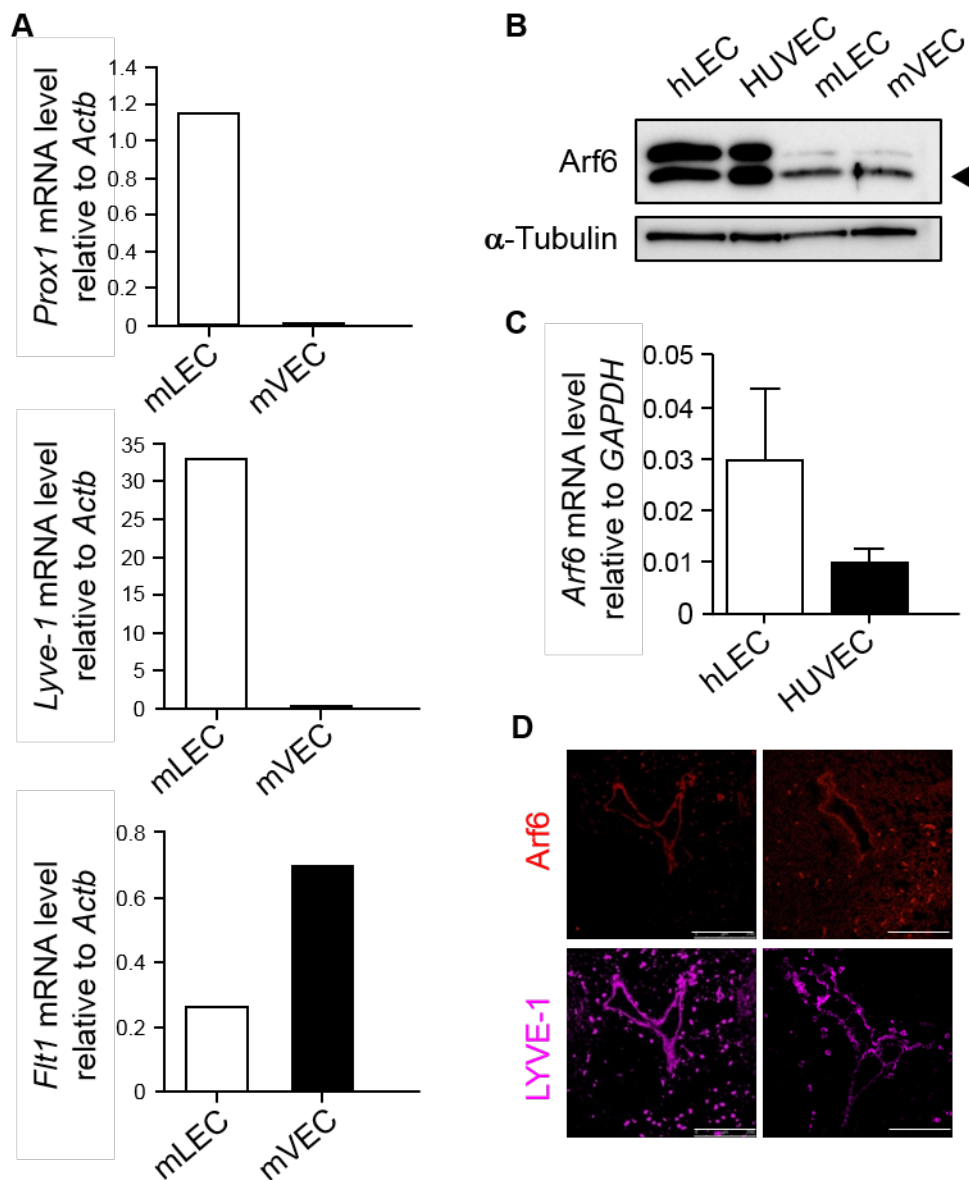
Figure 11. Arf6 is expressed in mLECs

(A) Verification of mLECs and mVECs purified from E16.5 embryos by qRT-PCR for the lymphatic markers *Prox1* and *Lyve-1*, and the blood vessel marker *Flt1*. (B) The expression levels of Arf6 protein in hLECs, HUVECs, mLECs, and mVECs determined by Western blotting. (C) *Arf6* mRNA expression levels in hLECs and HUVECs analyzed by qRT-PCR. The data were shown as mean ± SEM from three independent experiments. Statistical significance was assessed using unpaired Student's *t*-test. *$P < 0.05$. (D) Expression of Arf6 (red) in LYVE-1-positive transverse jugular lymph sacs (purple) of E13.5 mouse embryos. Scale bars, 200 μm.

The defect of lymphangiogenesis observed in *Arf6*^{-/-} embryos and the expression of Arf6 in mLECs led us to hypothesize that Arf6 in mLECs functions in development lymphangiogenesis. To test this hypothesis, we generated LEC-*Arf6* cKO mice. Arf6 would be successfully deleted from mLECs in LEC-*Arf6* cKO mice since the tdsRed signal was detected in the lymphatic vessels of *R26GRR;Prox1-CreER;Arf6*^{flox/+} mice treated with tamoxifen (Figure 12). Consistent with the results obtained with *Arf6*^{-/-} mice, E15.5 LEC-*Arf6* cKO mice showed edema, delay of the lymphatic vessel extension, and defects in the branch points, vessel length and vessel width (Figure 10D-F). The phenotypes observed in *Arf6*^{-/-} and LEC-*Arf6* cKO embryos were not due to the defect in blood vessel formation as was shown in Figure 13. Although heart development disorder is known to cause embryonic edema, LEC-*Arf6* cKO embryos did not show any heart defect in the histological analysis (Figure 14). Taken together, these results strongly suggest that Arf6 in mLECs is essential for the developmental lymphangiogenesis.
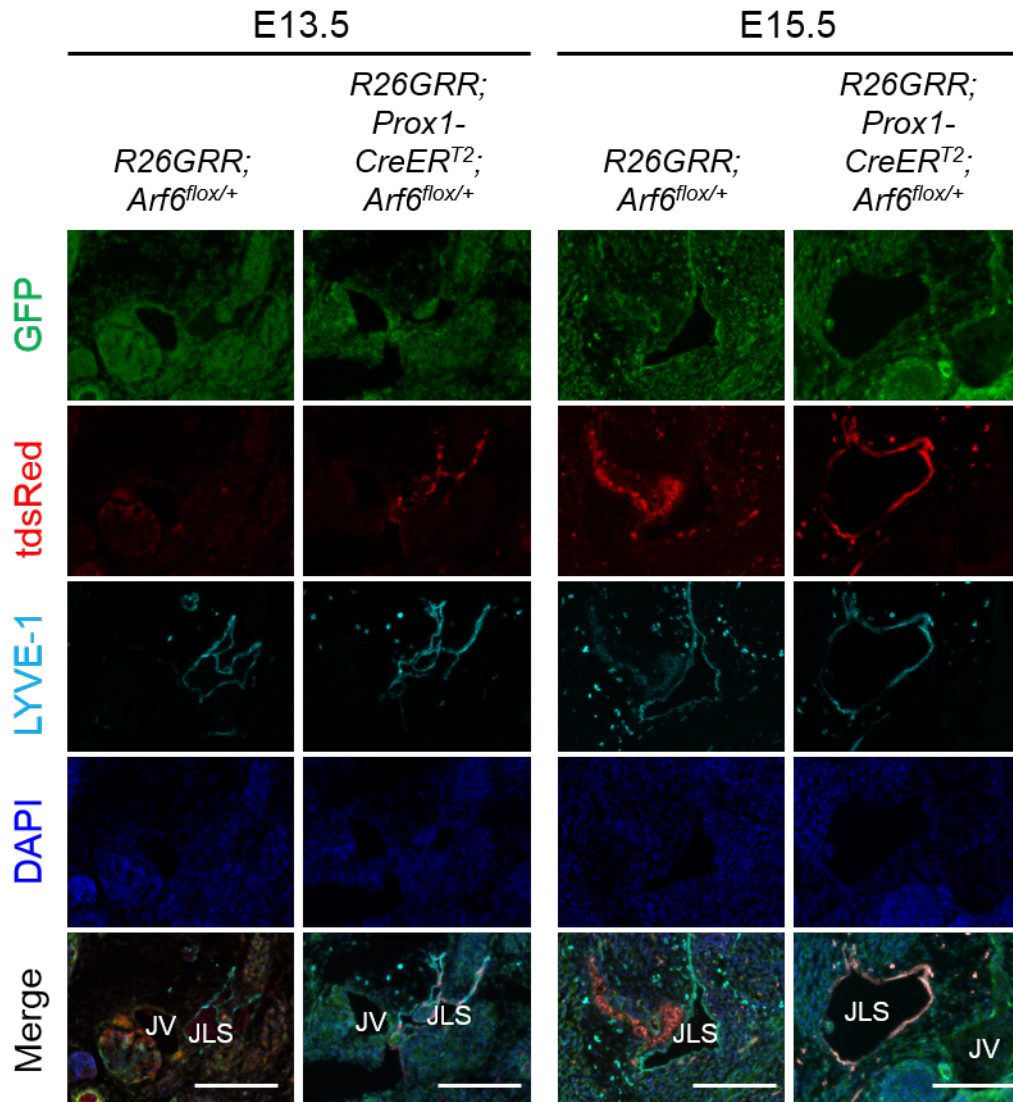
Figure 12. Cre recombinase expression in mLECs of the jugular lymph sac

Transverse jugular sections prepared from E13.5 and E15.5 GFP-expressing control *R26GRR;Arf6^flox/+^* and *R26GRR;Prox1-CreER^T2^;Arf6^flox/+^* embryos, which were administrated with tamoxifen, were stained for LYVE-1 (cyan) and DAPI (blue). tdsRed signal (red) indicates the tamoxifen-stimulated Cre recombinase activity. JLS, jugular lymph sac. JV, jugular vein. Scale bars, 200 μm.
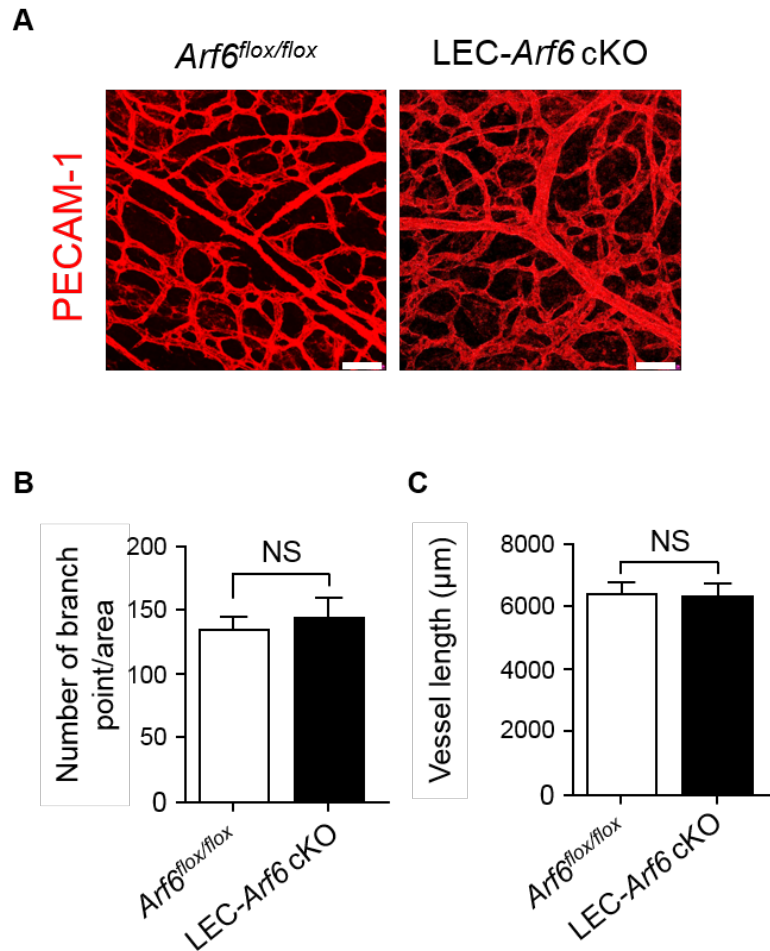
Figure 13. mLEC-specific *Arf6* knockout does not impair the blood vessel formation. (A) Confocal z-stack images of dorsal view of subcutaneous blood vessels stained for PECAM-1 in E15.5 control *Arf6^flox/flox^* and LEC-*Arf6*-cKO embryos. (B) Quantification of branch points of blood vessels/area (393 × 393 μm) in control *Arf6^flox/flox^* (n = 3) and LEC-*Arf6*-cKO (n = 3) embryos. (C) Quantification of total blood vessel length/area (393 × 393 μm) in control *Arf6^flox/flox^* (n = 3) and LEC-*Arf6*-cKO (n = 3) embryos. The data shown were the mean ± SEM from at least three independent experiments. Statistical significance was assessed using Student's *t*-test. NS, not significant. Scale bar, 50 μm.
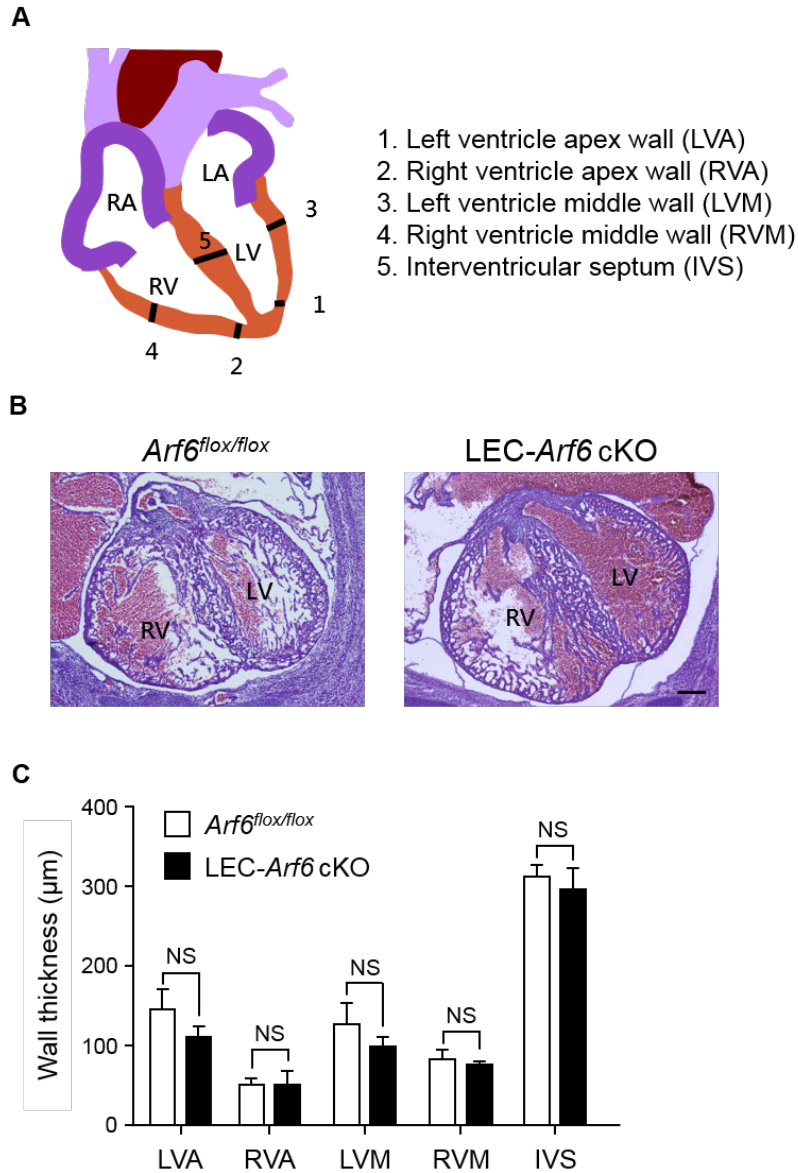
Figure 14. LEC-*Arf6* cKO mice do not show heart failure. (A) Schematic anatomy of the heart in E15.5 embryos. LA, left atrium. LV, left ventricle. RA, right atrium. RV, right ventricle. (B) Hematoxylin & Eosin staining of transverse heart sections of E15.5 control *Arf6*^{flox/flox} and LEC-*Arf6*-cKO embryos. (C) Quantification of the thickness of left ventricle apex wall (LVA), right ventricle apex wall (RVA), left ventricle middle wall (LVM), right ventricle middle wall (RVM) and interventricular septum (IVS) in E15.5 control *Arf6*^{flox/flox} and LEC-*Arf6*-cKO embryos. The data shown are mean ± SEM from at least three independent experiments. Statistical significance was assessed using Student's *t*-test. NS, not significant. Scale bar, 200 μm.

Arf6 plays a role in the formation of lymph sacs

To examine the functions of Arf6 in an early event of developmental lymphangiogenesis, we analyzed primary lymph sac formation. In E13.5 and E15.5 LEC-*Arf6* cKO embryos, LYVE-1$^+$ and PECAM-1$^+$ lymph sacs were enlarged compared with those in control *Arf6$^{flox/flox}$* embryos (Figure 15).
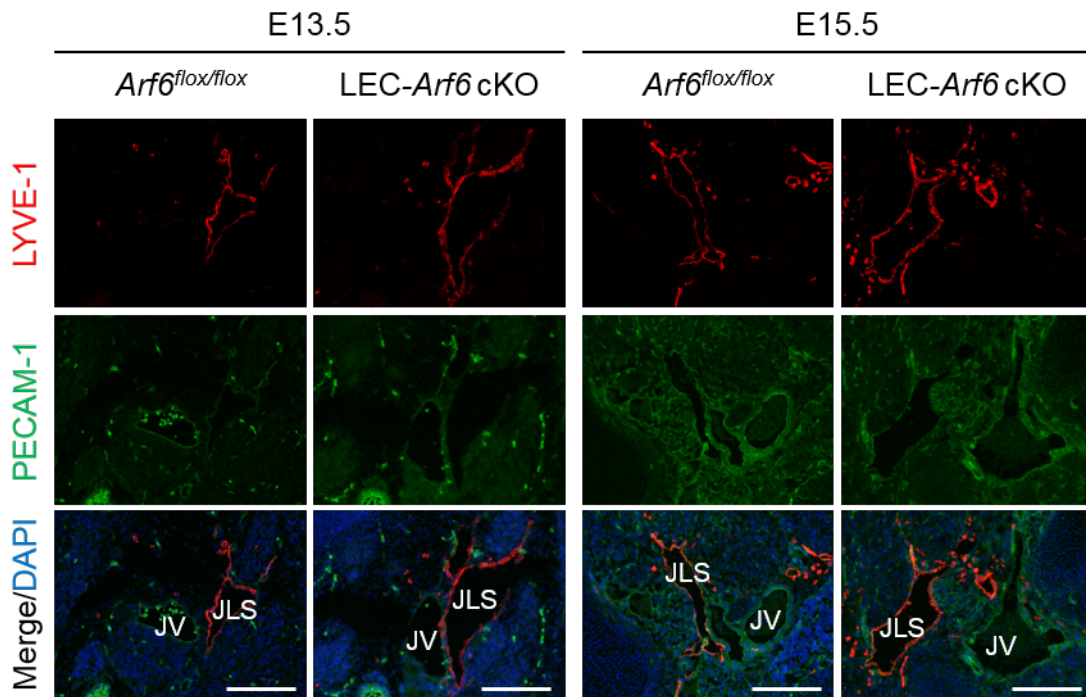
Figure 15. Jugular lymph sacs enlarge in LEC-*Arf6* cKO mice

Transverse jugular sections of E13.5 and E15.5 control *Arf6$^{flox/flox}$* and LEC-*Arf6*-cKO embryos were immunostained for LYVE-1 (red), PECAM-1 (green) and DAPI (blue). Note that the LYVE-1 positive JLS in LEC-*Arf6* cKO embryos enlarged compared with that in control embryos. JV, jugular vein. JLS, jugular lymph sac. Scale bar, 200 μm.

Sprouting of the lymphatic vessel from lymph sacs is the second step in the developmental lymphangiogenesis to form the lymphatic vascular network. Arf6 appeared to play a function in the sprouting of lymphatic vessels, since LEC-*Arf6* cKO embryos lacked any sprouting tips and showed enlarged LYVE-1^{+} and Prox1^{+} lymphatic vessels (Figure 16A). The enlargement of lymphatic vessels was not due to the enhancement of mLEC proliferation as assessed by immunostaining of developing lymphatic vessels for the proliferation marker Ki67 (Figure 17B). This result was supported by the finding that knockdown of Arf6 in hLECs was without effects on hLEC proliferation *in vitro* (Figure 17). Moreover, it was found that the nuclei of mLECs in LEC-*Arf6* cKO embryos were spherical, while those of control mLECs were oval (Figure 16C), suggesting that Arf6 regulates sprouting by controling the cell migration. These results demonstrate that Arf6 in mLECs plays an important role in sprouting from the lymph sac to form the lymphatic vascular network.
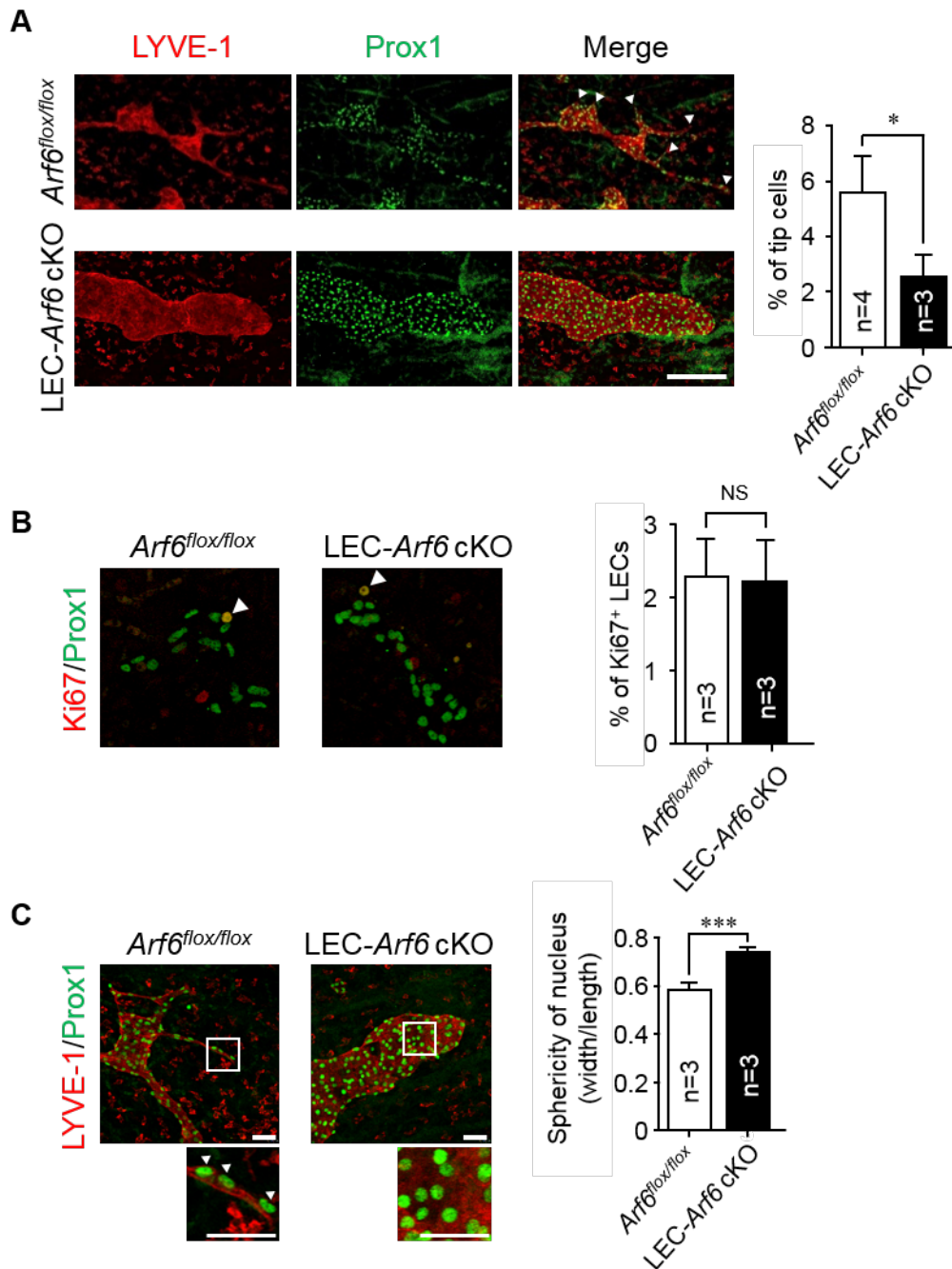
Figure 16. Arf6 regulates lymphatic vessel sprouting and tip cell morphology
(A) Representative images of sprouting lymphatic vessels in E15.5 control
Arf6flox/flox (n = 4) and LEC-*Arf6* cKO (n = 3) (left panels). Transverse jugular
sections were co-immunostained for LYVE-1 (red) and Prox1 (green). Arrowheads
indicate sprouts of lymphatic vessels. Immunostained images shown in the left
panels were quantified for the number of Prox1^{+} lymphatic tip cells in the distal
migration front area of lymphatic vessels (right panel). Scale bar, 200 μm. (B)
Representative images of proliferating mLECs in the subcutaneous lymphatic

32

vessel of E15.5 control *Arf6flox/flox* (n = 5) and LEC-*Arf6* cKO (n = 5) embryos co-immunostained for Prox1 (green) and Ki67 (red) (left panels). Arrowheads represent Prox1$^+$/Ki67$^+$ proliferating mLECs (left panel). Percentages of Prox1$^+$/Ki67$^+$ proliferative mLECs of total Prox1$^+$ mLECs in the distal migrating front area of lymphatic vessels were quantified (right panel). (C) Representative images of subcutaneous lymphatic vessels in E15.5 control *Arf6flox/flox* (n = 3) and LEC-*Arf6*-cKO embryos (n = 3) co-immunostained for LYVE-1 (red) and Prox1 (green). Lower panels are magnified images of the square area in the upper panels. Arrowheads in the magnified images indicate the oval nucleus. Immunostained images were quantified for sphericity of nucleus (width/length) (right panel). Statistical significance was assessed using student's *t*-test. NS, not significant, *P < 0.05, ***P < 0.005. Scale bar, 200 μm (A, B) and 25 μm (C).
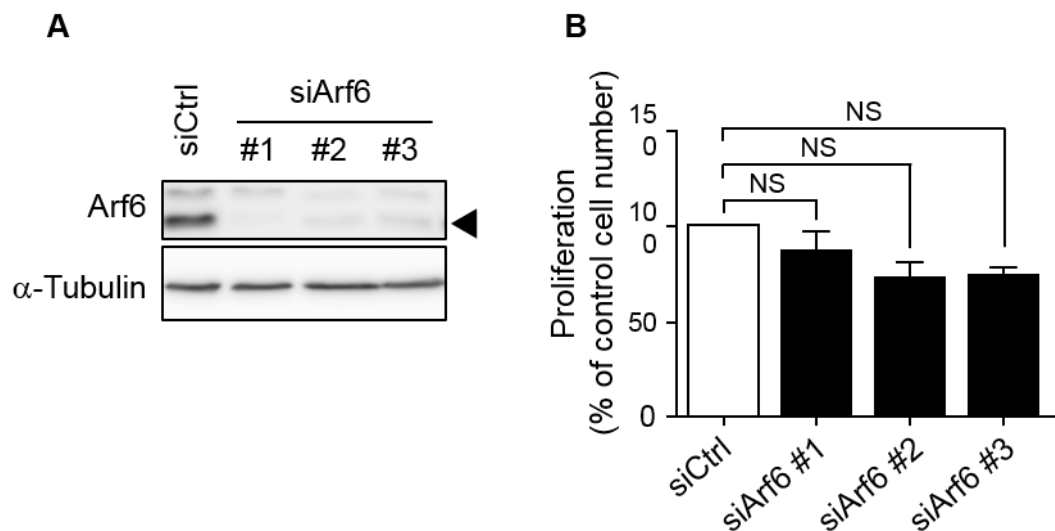
Figure 17. Arf6 is not involved in cell proliferation of hLECs

(A) Knockdown of Arf6 in hLECs. (B) Effect of Arf6 knockdown on the cell proliferation of hLECs. After two days of cell culture, cell number was counted. The data shown are mean ± SEM from five independent experiments. Statistical significance was assessed using One-way ANOVA. NS, not significant.

Arf6 in mLECs promotes in vitro capillary tube formation by regulating cell migration upon VEGF-C stimulation

It has been reported that VEGF-C signaling regulates lymphatic vascular development [138]. To address a question whether Arf6 regulates VEGF-C-dependent lymphatic vascular formation, we investigated the involvement of Arf6 on the VEGF-C-dependent *in vitro* capillary tube formation by hLECs. As was expected, knockdown of Arf6 in hLECs (Figure 17) impaired the VEGF-C-induced tube formation (Figure 18A).

Since VEGF-C signaling regulates migration of LECs [138, 139], which is an essential cell event for lymphatic vascular development, we examined whether Arf6 regulates hLEC migration by wound healing and transwell migration assays. At 24 hr after wounding, the VEGF-C-dependent wound closure was significantly delayed in Arf6-knocked-down hLECs (~40% closure) compared with control (~75% closure) (Figure 18B). Transwell migration of hLECs using VEGF-C as a chemoattractant was also markedly inhibited by knockdown of Arf6 (Figure 18C). Thus, Arf6 appeared to play an important role in the cell migration.
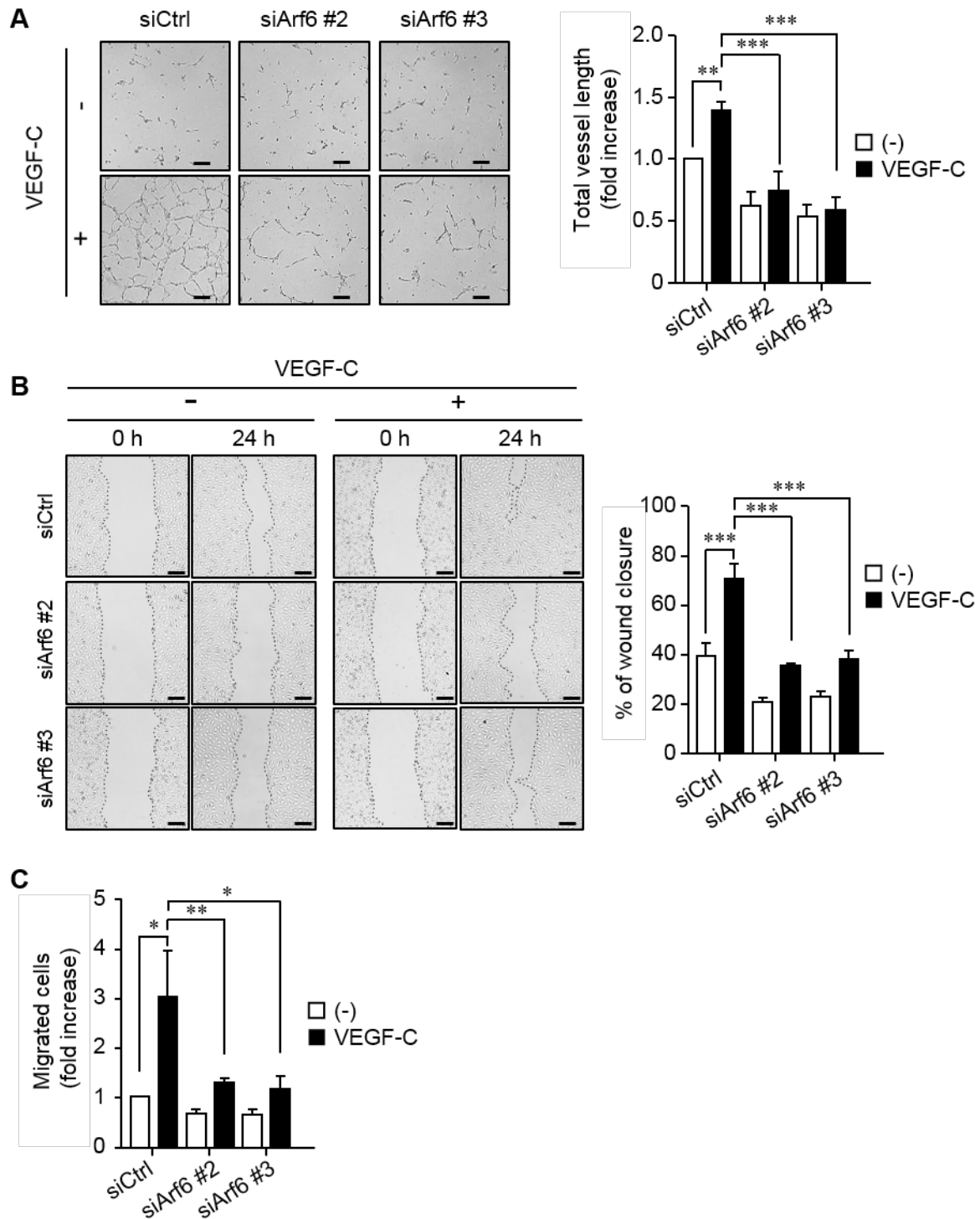
Figure 18. Arf6 regulates *in vitro* capillary tube formation and cell migration of hLECs

(A) Representative images of *in vitro* capillary tube formation by control and Arf6-knocked-down hLECs (left panels), and quantified data for total tube length (right panel). The control and Arf6-knocked-down hLECs were stimulated without or with 200 ng/ml of VEGF-C for 24 hr. Total vessel length was calculated in 4

fields/experiments of three independent experiments. (B) Representative images of wound healing by control and Arf6-knocked-down hLECs (left panels), and quantified data for percentages of wound closure (right panel). Confluent monolayers of hLECs transfected with control and *Arf6* siRNAs were scratched and immediately treated without or with 200 ng/ml of VEGF-C, and images were obtained at 0 and 24 hr after wounding. Dotted lines in the images indicate the border of the wound. Wound closure was measured in 4 fields/experiment of four independent experiments and represented as percentages of wound distance during 24 hr. (C) Cell migration of control and *Arf6*-knocked-down hLECs stimulated without or with 200 ng/ml of VEGF-C. Cells migrated to the lower surface of the membrane filter in transwell migration chamber were stained with DAPI. DAPI-positive cells in four fields per sample were counted, and the data were shown as means ± SEM from at least 3 independent experiments. Statistical significance was assessed using one-way ANOVA. *$P < 0.05$, **$P < 0.01$, ***$P < 0.005$. Scale bar, 200 μm.

Arf6 regulates directional cell migration of LECs

To further investigate whether Arf6 regulates the directional cell migration, time-lapse tracking of hLEC movement in response to VEGF-C stimulation was analyzed (Figure 19A). Although knockdown of Arf6 did not affect accumulated distance, euclidean distance and directionality of cells were significantly reduced by Arf6 knockdown (Figure 19B). Thus, Arf6 is required for the directional cell migration but not for unsophisticated cell movement.

Interference with the directed cell migration by Arf6 knockdown may be resulted from the disturbance of cell polarity, since Golgi orientation, which has been shown to be involved in the cell polarity [136, 137, 140], was randomized in Arf6-knocked-down hLECs (Figure 19C): although migrating control cells at the wounded site elongated (left top panel, arrow heads), Arf6-knocked-down cells remained spherical (middle and right top panels), which is consistent with the results shown in Figure 16C that the nuclei of mLECs in LEC-*Arf6* cKO embryos showed spherical shape while those of control mLECs was oval. Taken together, these results suggest that Arf6 in LECs regulates directional cell migration by controlling cell polarity.

36
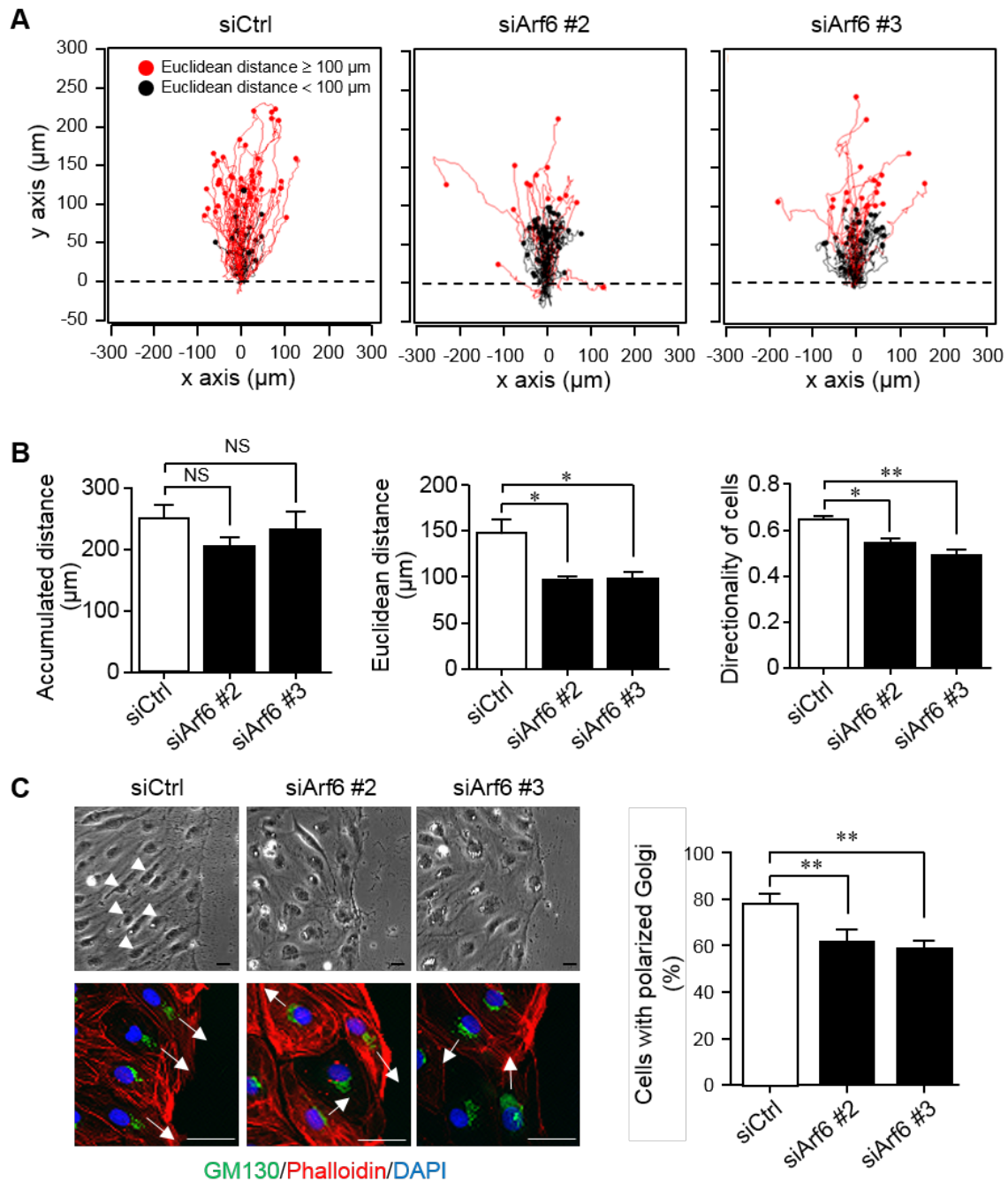
Figure 19. Arf6 knockdown causes defect in directed cell migration of hLECs.
(A) Tracking of cell migration during wound healing by time-lapse video microscopy. Control and Arf6-knocked-down hLECs were grown to the confluence, scratched, and stimulated with 200 ng/ml of VEGF-C. Images were obtained every 10 min for 20 hr after wounding. Each line represents the trajectory of an individual cell. Red and black lines indicate the euclidean distance over and less than 100 μm, respectively. Dotted lines indicate the boarder of the wound. Each experiment was performed four times, and at least 60 cells per experiment were analyzed. (B)

Images shown in (A) were quantified for accumulated distance (left panel), euclidean distance (middle panel), and directionality (right panel), which was calculated by dividing euclidean distance by accumulated distance. (C) Representative phase contrast microscopic images of control and Arf6-knocked-down of hLECs (upper images) and immunostained images with anti-GM130 antibody (green), phalloidin (red), and DAPI (blue) (lower images) at the wounded edge (left panels). Arrowheads indicate elongated cells. Arrows indicate the migrating direction of the cell as decided by the location of Golgi. Images were quantified for cells with polarized Golgi (right panel). At least 200 cells per experiment were analyzed, and data were shown as means ± SEM from at least 3 independent experiments. Statistical significance was assessed using one-way ANOVA. NS, not significant, *P < 0.05, **P < 0.01. Scale bar, 25 μm.

Arf6 regulates internalization of β1 integrin in LECs

Impairment of the internalization of cell surface β1 integrin in nascent endothelium disrupts arterial endothelial cell polarity and lumen formation [141-143]. In addition, it has been reported that Arf6 signaling regulates the internalization of β1 integrin [144, 145]. These reports led us to examine whether Arf6 is involved in the β1 integrin internalization in LECs. The total amount of β1 integrin in hLECs was not affected by knockdown of Arf6 (Figure 20A). When the levels of active form of surface β1 integrin and the adhesion molecule paxillin were analyzed, levels of both molecules were significantly increased in Arf6-knocked-down hLECs (Figure 20B). In addition, β1 integrin internalization promoted by VEGF-C stimulation of hLECs in a time-dependent manner was almost completely inhibited by knockdown of Arf6 (Figure 20C). These results, taken together, suggest that Arf6 regulates VEGF-C-induced cell polarity and directional cell migration by controling β1 integrin internalization in LECs.
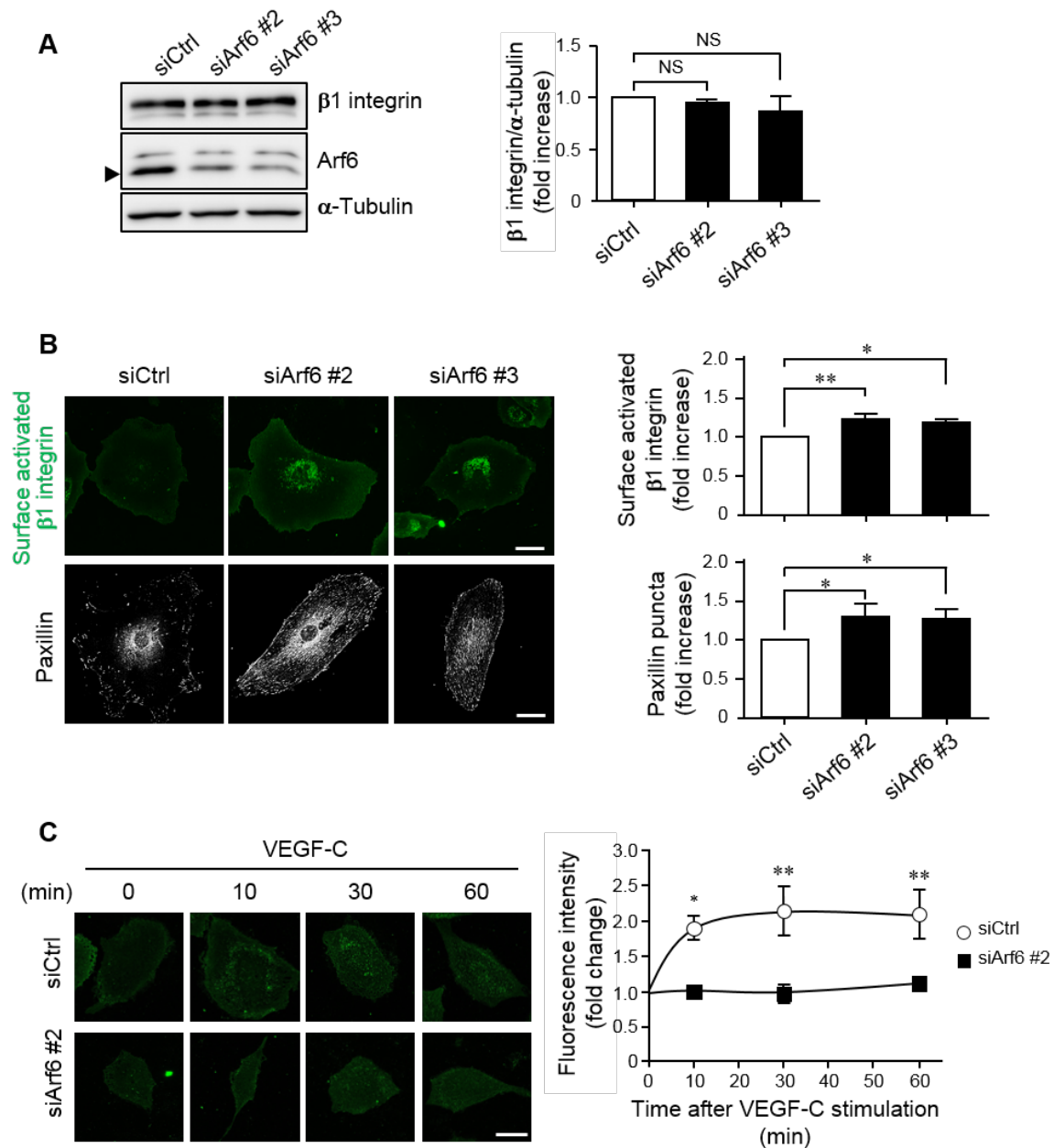
Figure 20. Arf6 regulates β1 integrin internalization in hLECs. (A) Western blots of β1 integrin levels in control and Arf6-knocked-down hLECs (left panel), and their quantified data (right panel). (B) Representative images of surface activated β1 integrin (green, upper panels) and paxillin (white, lower panels) in control and Arf6-knocked-down hLECs (left panels), and quantified data for their levels (right panels). (C) Representative images of time-dependent β1 integrin internalization (left panels) and its quantified data (right panel). The internalized β1 integrin was shown in green. Data were shown as means ± SEM from at least 3 independent experiments. Statistical significance was assessed using One-way

ANOVA. NS, not significant, * $P < 0.05$, **$P < 0.01$. Scale bar, 25 μm (B) and 50 μm (C).

Ablation of Arf6 from LECs interferes with tumor lymphangiogenesis and cancer progression

Cancer progression and lymphatic metastasis are tightly related with tumor lymphangiogenesis [146, 147]. These reports and the results shown above raised a possibility that Arf6 in LECs is involved in tumor lymphangiogenesis and cancer progression. To address these issues, B16 melanoma cells were transplanted into tamoxifen-treated LEC-*Arf6* cKO mice (Figure 21A). The tumor volume produced was significantly reduced by knockout of *Arf6* in mLECs (Figure 21B,C). Correlated to this result, tumor lymphangiogenesis was suppressed by *Arf6* knockout (Figure 22). Thus, Arf6 in mLECs plays an important role in tumor lymphangiogenesis, thereby regulating cancer progression. These results provide a new cancer therapeutic opportunity.
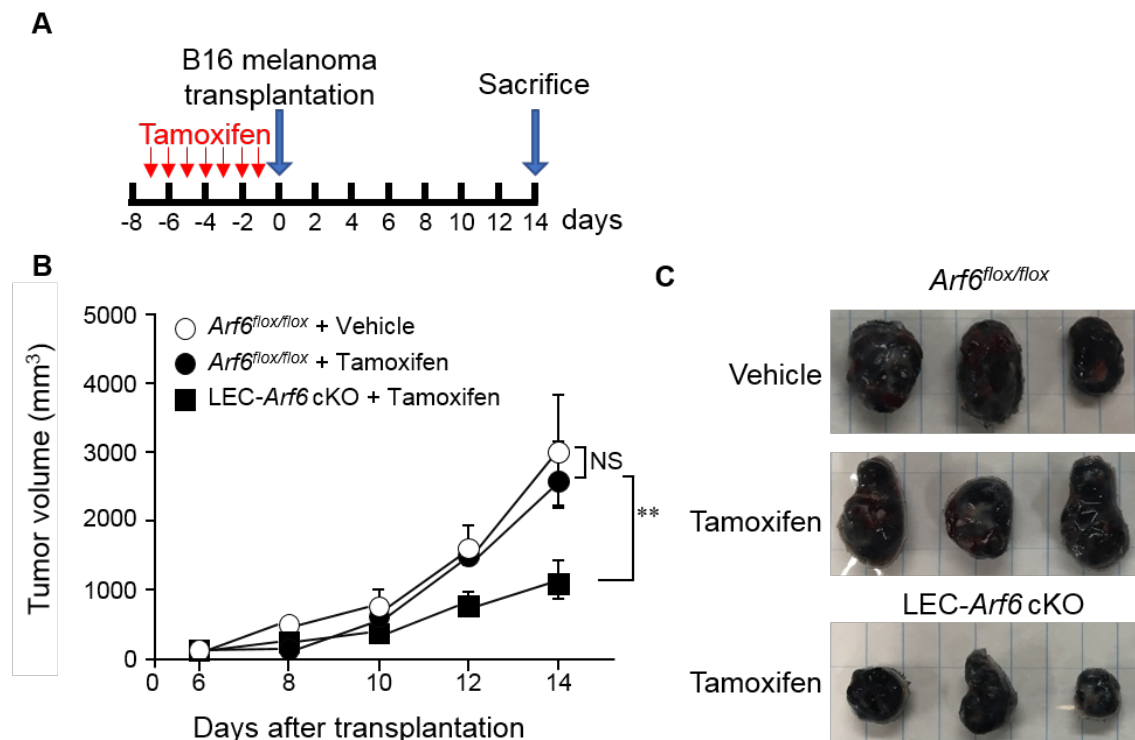
Figure 21. The effect of Arf6 ablation from LECs on tumor progression

Scheme of the assay for the effect of Arf6 ablation from mLECs on tumor progression. Tamoxifen (3 mg) was daily injected into the peritoneal cavity of the

mice for one week, and B16 melanoma cells (2×10^4 cells) were subcutaneously transplanted into the right lower back region of the mice. The size of the tumor was measured by digital caliper every two days from day 6 after the transplantation. (B) Tumor volumes produced in vehicle-treated $Arf6^{flox/flox}$, tamoxifen-treated $Arf6^{flox/flox}$, and tamoxifen-treated LEC-$Arf6$ cKO mice were measured according to the schedule described in (A). (C) At 14 days of the transplantation, tumors were dissected, and 3 examples were shown. The data shown in (B) are mean ± SEM from three independent experiments. Statistical significance was assessed using One-way ANOVA. NS, not significant. $**P < 0.01$.
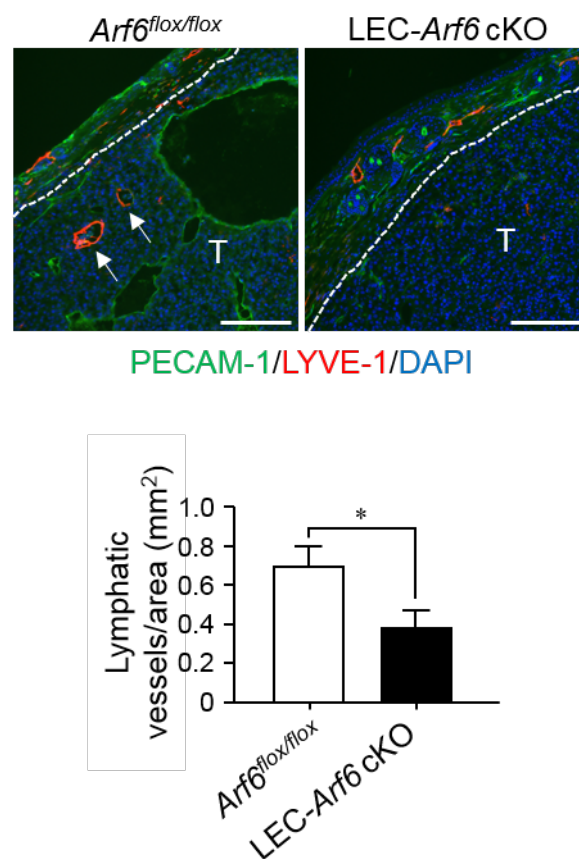
Figure 22. Arf6 in mLECs positively regulates tumor lymphangiogenesis. Representative images of lymphatic vessels in B16 melanoma tumors produced in control $Arf6^{flox/flox}$ (n = 3) and LEC-$Arf6$ cKO mice (n = 3). Tumor sections were co-immunostained for LYVE-1 (red) and PECAM1 (green) (upper panels). Arrows and the letter T indicate the lymphatic vessel and the tumor, respectively. White

dashed lines are the border between the tumor and dermis. Quantification of percentages of lymphatic vessels/area (1525×1140 µm area) (lower panel) was calculated in 10 fields of images/experiments. Data shown were the mean ± SEM from at least 3 independent experiments. Statistical significance was assessed using student's *t*-test, *$P < 0.05$. Scale bar, 200 µm.

Discussion

The results obtained in this study demonsrate for the first time that the small G protein Arf6 in LECs plays an important role in the VEGF-C-induced directional cell migration, which is critical for lymphatic vascular network formation, by regulating β1 integrin internalization, providing insight into the molecular mechanism of developmental lymphangiogenesis. Furthermore, we clarified that Arf6 in LECs plays pivotal roles in tumor lymphangiogenesis and cancer progression, giving a new cancer therapeutic opportunity. Thus, our findings in this study provide insight into not only physiological but also pathological functions of Arf6 in LECs.

Although Arf6 has been well established to regulate the integrin recycling [58, 144, 148], the molecular mechanisms for VEGF-C-dependent Arf6-mediated β1 integrin recycling in LECs still remained unclear. Activation of Arf6 in LECs in response to VEGF-C stimulation could be essential for the integrin recycling. This assumption is supported by the report that the Arf6-specific GEF GEP100 promotes the β1 integrin endocytosis to enhance the cell attachment to and spreading on the β1 integrin substrate fibronectin [144]. Recently, we have reported that Arf6 is activated by the GTPase dynamin2, which promotes scission of the invaginated plasma membrane in a manner dependent on its conformational change induced upon GTP hydrolysis [149]. The Arf6 activation by dynamin2 is mediated by the Arf6-specific GEFs such as EFA6A, EFA6B, and EFA6D during clathrin-mediated endocytosis [149]. If it is the case that these Arf6 GEFs are involved in VEGF-C-stimulated Arf6 activation in LECs, dynamin2 mediates VEGF-C-dependent Arf6 activation through an Arf6 GEF(s). This issue remains to be clarified.

What is the cellular signaling downstream of the activated Arf6 coupling to the β1 integrin endocytosis in VEGF-C-stimiulated LECs? It is plausible that the lipid kinase PIP5K, which is directly activated by the active form of Arf6 to produce the versatile signaling lipid PI(4,5)P$_2$ at the plasma membrane [21], is involved in this cellular signaling as an effector molecule of Arf6 activated by VEGF-C stimulateion. The PIP5K product PI(4,5)P$_2$ regulates activities of actin-binding proteins such as the actin severing and capping protein gelsolin, thereby reorganizing actin cytoskeleton to facilitate endocytosis of membrane proteins [150-152]. Alternatively, PLD1 which produces the signaling lipid PA may function as a mediator for the active form of Arf6 coupling to β1 integrin endocytosis. This idea is derived from the reports that PLD1 is directly activated by Arf6 in response to agonist stimulation [153, 154], and its product PA facilitates endocytosis by forming the membrane curvature at

the neck of the deeply invaginated membrane [155, 156]. In addition to these possible functions of PIP5K and PLD1 in β1 integrin endocytosis, these two lipid-metabolizing enzymes mutually accelerate their activation by a positive feedback mechanism: PA is necessary for the activation of PIP5K by Arf6 [156], and PI(4,5)P$_2$ supports PLD1 activation by Arf6 [157].

Besides Arf6, other proteins may be involved in VEGF-C-stimulated β1 integrin endocytosis to regulate directional cell migration. For example, the endocytic adaptor protein Numb has been reported to bind β1 integrin and control integrin endocytosis for directional cell migration with aPKC and PAR-3 [158]. Thus, the molecular mechanism of β1 integrin endocytosis seems to be very complicated, and it is of interest to clarify the precise molecular mechanism for VEGF-C-dependent β1 integrin endocytosis, especially crosstalk of cellular signaling pathways in this cell event.

Interestingly, it has been reported that in a model mouse of hypotrichosis-lymphedema-telangiectasia, *Ragged Opossum*, the Arf6 GAP ARAP3 in lymphatic vessels that is necessary for lymphatic vascular development is down-regulated [159]. Furthermore, this report demonstrated that *Arap3*$^{-/-}$ embryos show the lymphatic vascular network deficiency with enlarged lymphatic vessels, which are the same phenotypes observed in *Arf6*$^{-/-}$ and LEC-*Arf6* cKO mice (Figure 10). These observations indicate that appropriate cycling of Arf6 between activation and inactivation that are precisely regulated by Arf6-specific GEFs and GAPs, respectively, is essential for the development of dermal lymphatic vasculature network. This idea is consistent with our recent report demonstrating that cycling between active and inactive states of Arf6 is required for promoting neurite outgrowth [160].

The edema on the back of *Arf6*$^{-/-}$ mice was observed at E13.5 (Figure 10A), while LEC-*Arf6* cKO embryos showed the edema at E15.5 but not at E13.5 (Figure 10D). This difference in the embryonic days inducing edema between these two types of *Arf6*-deficient mice would be attributable to the involvement of another type(s) of cells distinct from LECs in an earlier step of lymphangiogenesis. This idea is supported by the report that the lymphatic vascular system predominantly originates from the vein at earlier stage of development (E7.5) before lymphatic vessels are formed at E9.5 in mouse embryos [161]. Moreover, it has been reported that non-venous mesenchymal cells also contribute to an earlier step(s) of lymphatic development as a source of LECs [162]. These observations explain well why we did not observe any defects in the lymphatic vessel formation in the

VEC-specific *Arf6* cKO mice (data not shown), which had been generated previously [60], and why the edema was induced in *Arf6*$^{-/-}$ embryos earlier than in LEC-*Arf6* cKO embryos: ablation of *Arf6* from both venous and non-venous mesenchymal cells in *Arf6*$^{-/-}$ embryos might induce the lymphedema earlier than LEC-*Arf6*-cKO.

Finally, we demonstrated in this study that Arf6 in LECs is a key molecule for tumor lymphangiogenesis and cancer progression (Figure 21 and Figure 22). Tumor lymphangiogenesis, as well as tumor angiogenesis, is a potential therapeutic target for cancer treatment [153, 154]. We have recently reported that Arf6 expressed in VECs plays an important role in tumor angiogenesis and cancer progression: ablation of *Arf6* from mVECs inhibits tumor angiogenesis, therefore suppressing tumor growth [60]. Thus, Arf6 in pan-endothelial cells is a highly potential therapeutic target to prevent cancer progression. However, recent preclinical studies have suggested that anti-angiogenic therapy promotes cancer metastasis by inducing hypoxia in cancer cells [163, 164]. It is noteworthy that Arf6 expressed in breast cancer cells is required for cancer metastasis [34]. Thus, Arf6 plays critical roles in tumor lymphangiogenesis/angiogenesis and cancer metastasis. These reports and our results obtained in this study suggest that an inhibitor(s) of Arf6 could efficiently prevent both tumor progression and metastasis. Specific inhibitors of Arf6 might provide a new cancer therapeutic opportunity.

References

1. Takai, Y., T. Sasaki, and T. Matozaki, *Small GTP-binding proteins.* Physiol Rev, 2001. **81**(1): p. 153-208.

2. Kahn, R.A. and A.G. Gilman, *The protein cofactor necessary for ADP-ribosylation of Gs by cholera toxin is itself a GTP binding protein.* J Biol Chem, 1986. **261**(17): p. 7906-11.

3. Chavrier, P. and B. Goud, *The role of ARF and Rab GTPases in membrane transport.* Curr Opin Cell Biol, 1999. **11**(4): p. 466-75.

4. D'Souza-Schorey, C. and P. Chavrier, *ARF proteins: roles in membrane traffic and beyond.* Nat Rev Mol Cell Biol, 2006. **7**(5): p. 347-58.

5. Kahn, R.A., et al., *Nomenclature for the human Arf family of GTP-binding proteins: ARF, ARL, and SAR proteins.* J Cell Biol, 2006. **172**(5): p. 645-50.

6. Bonifacino, J.S., *The GGA proteins: adaptors on the move.* Nat Rev Mol Cell Biol, 2004. **5**(1): p. 23-32.

7. Claude, A., et al., *GBF1: A novel Golgi-associated BFA-resistant guanine nucleotide exchange factor that displays specificity for ADP-ribosylation factor 5.* J Cell Biol, 1999. **146**(1): p. 71-84.

8. Takatsu, H., et al., *GGA proteins associate with Golgi membranes through interaction between their GGAH domains and ADP-ribosylation factors.* Biochem J, 2002. **365**(Pt 2): p. 369-78.

9. D'Souza-Schorey, C., et al., *A regulatory role for ARF6 in receptor-mediated endocytosis.* Science, 1995. **267**(5201): p. 1175-8.

10. Peters, P.J., et al., *Overexpression of wild-type and mutant ARF1 and ARF6: distinct perturbations of nonoverlapping membrane compartments.* J Cell Biol, 1995. **128**(6): p. 1003-17.

11. Donaldson, J.G. and C.L. Jackson, *ARF family G proteins and their regulators: roles in membrane transport, development and disease.* Nat Rev Mol Cell Biol, 2011. **12**(6): p. 362-75.

12. Antonny, B., et al., *N-terminal hydrophobic residues of the G-protein ADP-ribosylation factor-1 insert into membrane phospholipids upon GDP to GTP exchange.* Biochemistry, 1997. **36**(15): p. 4675-84.

13. Chavrier, P. and J. Menetrey, *Toward a structural understanding of arf family:effector specificity.* Structure, 2010. **18**(12): p. 1552-8.

14. Hongu, T. and Y. Kanaho, *Activation machinery of the small GTPase Arf6.* Adv Biol Regul, 2014. **54**: p. 59-66.

15. Casanova, J.E., *Regulation of Arf activation: the Sec7 family of guanine nucleotide exchange factors.* Traffic, 2007. **8**(11): p. 1476-85.

16. Derrien, V., et al., *A conserved C-terminal domain of EFA6-family ARF6-guanine nucleotide exchange factors induces lengthening of microvilli-like membrane protrusions.* J Cell Sci, 2002. **115**(Pt 14): p. 2867-79.

17. Franco, M., et al., *EFA6, a sec7 domain-containing exchange factor for ARF6, coordinates membrane recycling and actin cytoskeleton organization.* EMBO J, 1999. **18**(6): p. 1480-91.

18. Someya, A., et al., *ARF-GEP(100), a guanine nucleotide-exchange protein for ADP-ribosylation factor 6.* Proc Natl Acad Sci U S A, 2001. **98**(5): p. 2413-8.

19. Brown, H.A., et al., *ADP-ribosylation factor, a small GTP-dependent regulatory protein, stimulates phospholipase D activity.* Cell, 1993. **75**(6): p. 1137-44.

20. Cockcroft, S., et al., *Phospholipase D: a downstream effector of ARF in granulocytes.* Science, 1994. **263**(5146): p. 523-6.

21. Honda, A., et al., *Phosphatidylinositol 4-phosphate 5-kinase α is a downstream effector of the small G protein ARF6 in membrane ruffle formation.* Cell, 1999. **99**(5): p. 521-32.

22. Krauss, M., et al., *ARF6 stimulates clathrin/AP-2 recruitment to synaptic membranes by activating phosphatidylinositol phosphate kinase type Iγ.* J Cell Biol, 2003. **162**(1): p. 113-24.

23. McDermott, M., M.J. Wakelam, and A.J. Morris, *Phospholipase D.* Biochem Cell Biol, 2004. **82**(1): p. 225-53.

24. Prescott, E.D. and D. Julius, *A modular PIP2 binding site as a determinant of capsaicin receptor sensitivity.* Science, 2003. **300**(5623): p. 1284-8.

25. Simonsen, A., et al., *The role of phosphoinositides in membrane transport.* Curr Opin Cell Biol, 2001. **13**(4): p. 485-92.

26. Siddhanta, A., et al., *Fragmentation of the Golgi apparatus. A role for β III spectrin and synthesis of phosphatidylinositol 4,5-bisphosphate.* J Biol Chem, 2003. **278**(3): p. 1957-65.

27. Godi, A., et al., *ADP ribosylation factor regulates spectrin binding to the Golgi complex.* Proc Natl Acad Sci U S A, 1998. **95**(15): p. 8607-12.

28. Yin, H.L. and P.A. Janmey, *Phosphoinositide regulation of the actin cytoskeleton.* Annu Rev Physiol, 2003. **65**: p. 761-89.

29. Irvine, R.F., *Nuclear lipid signalling.* Nat Rev Mol Cell Biol, 2003. **4**(5): p. 349-60.

30. Perez-Mansilla, B., et al., *The differential regulation of phosphatidylinositol 4-phosphate 5-kinases and phospholipase D1 by ADP-ribosylation factors 1 and 6.* Biochim Biophys Acta, 2006. **1761**(12): p. 1429-42.

31. Tanabe, K., et al., *Involvement of a novel ADP-ribosylation factor GTPase-activating protein, SMAP, in membrane trafficking: implications in cancer cell biology.* Cancer Sci, 2006. **97**(9): p. 801-6.

32. Li, J., et al., *An ACAP1-containing clathrin coat complex for endocytic recycling.* J Cell Biol, 2007. **178**(3): p. 453-64.

33. Sabe, H., *Requirement for Arf6 in Cell Adhesion, Migration, and Cancer Cell Invasion.* Journal of Biochemistry, 2003. **134**(4): p. 485-489.

34. Sabe, H., et al., *The EGFR-GEP100-Arf6-AMAP1 signaling pathway specific to breast cancer invasion and metastasis.* Traffic, 2009. **10**(8): p. 982-93.

35. Li, J., et al., *Phosphorylation of ACAP1 by Akt regulates the stimulation-dependent recycling of integrin beta1 to control cell migration.* Dev Cell, 2005. **9**(5): p. 663-73.

36. Onodera, Y., et al., *Expression of AMAP1, an ArfGAP, provides novel targets to inhibit breast cancer invasive activities.* EMBO J, 2005. **24**(5): p. 963-73.

37. Wolfe, B.L. and J. Trejo, *Clathrin-dependent mechanisms of G protein-coupled receptor endocytosis.* Traffic, 2007. **8**(5): p. 462-70.

38. Krishnan, K.S., et al., *Nucleoside diphosphate kinase, a source of GTP, is required for dynamin-dependent synaptic vesicle recycling.* Neuron, 2001. **30**(1): p. 197-210.

39. Palacios, F., et al., *ARF6-GTP recruits Nm23-H1 to facilitate dynamin-mediated endocytosis during adherens junctions disassembly.* Nat Cell Biol, 2002. **4**(12): p. 929-36.

40. Liu, L., et al., *SCAMP2 interacts with Arf6 and phospholipase D1 and links their function to exocytotic fusion pore formation in PC12 cells.* Mol Biol Cell, 2005. **16**(10): p. 4463-72.

41. Montagnac, G., et al., *ARF6 Interacts with JIP4 to control a motor switch mechanism regulating endosome traffic in cytokinesis.* Curr Biol, 2009. **19**(3): p. 184-95.

42. Prigent, M., et al., *ARF6 controls post-endocytic recycling through its downstream*

exocyst complex effector. J Cell Biol, 2003. **163**(5): p. 1111-21.

43. He, B. and W. Guo, *The exocyst complex in polarized exocytosis.* Curr Opin Cell Biol, 2009. **21**(4): p. 537-42.

44. Fielding, A.B., et al., *Rab11-FIP3 and FIP4 interact with Arf6 and the exocyst to control membrane traffic in cytokinesis.* EMBO J, 2005. **24**(19): p. 3389-99.

45. Man, Z., et al., *Arfaptins are localized to the trans-Golgi by interaction with Arl1, but not Arfs.* J Biol Chem, 2011. **286**(13): p. 11569-78.

46. Premont, R.T. and R. Schmalzigaug, *Metastasis: wherefore arf thou?* Curr Biol, 2009. **19**(22): p. R1036-8.

47. Martinu, L., et al., *The TBC (Tre-2/Bub2/Cdc16) domain protein TRE17 regulates plasma membrane-endosomal trafficking through activation of Arf6.* Mol Cell Biol, 2004. **24**(22): p. 9752-62.

48. Claing, A., et al., *β-Arrestin-mediated ADP-ribosylation factor 6 activation and β 2-adrenergic receptor endocytosis.* J Biol Chem, 2001. **276**(45): p. 42509-13.

49. Palacios, F., et al., *An essential role for ARF6-regulated membrane traffic in adherens junction turnover and epithelial cell migration.* EMBO J, 2001. **20**(17): p. 4973-86.

50. Claing, A., et al., *Multiple endocytic pathways of G protein-coupled receptors delineated by GIT1 sensitivity.* Proc Natl Acad Sci U S A, 2000. **97**(3): p. 1119-24.

51. Wenk, M.R. and P. De Camilli, *Protein-lipid interactions and phosphoinositide metabolism in membrane traffic: insights from vesicle recycling in nerve terminals.* Proc Natl Acad Sci U S A, 2004. **101**(22): p. 8262-9.

52. Paleotti, O., et al., *The small G-protein Arf6GTP recruits the AP-2 adaptor complex to membranes.* J Biol Chem, 2005. **280**(22): p. 21661-6.

53. Tanabe, K., et al., *A novel GTPase-activating protein for ARF6 directly interacts with clathrin and regulates clathrin-dependent endocytosis.* Mol Biol Cell, 2005. **16**(4): p. 1617-28.

54. Poupart, M.E., et al., *ARF6 regulates angiotensin II type 1 receptor endocytosis by controlling the recruitment of AP-2 and clathrin.* Cell Signal, 2007. **19**(11): p. 2370-8.

55. Eyster, C.A., et al., *Discovery of new cargo proteins that enter cells through clathrin-independent endocytosis.* Traffic, 2009. **10**(5): p. 590-9.

56. Maldonado-Baez, L., C. Williamson, and J.G. Donaldson, *Clathrin-independent endocytosis: a cargo-centric view.* Exp Cell Res, 2013. **319**(18): p. 2759-69.

57. Eyster, C.A., et al., *MARCH ubiquitin ligases alter the itinerary of clathrin-independent cargo from recycling to degradation.* Mol Biol Cell, 2011. **22**(17): p. 3218-30.

58. Powelka, A.M., et al., *Stimulation-dependent recycling of integrin β1 regulated by ARF6 and Rab11.* Traffic, 2004. **5**(1): p. 20-36.

59. Zimmermann, P., et al., *Syndecan recycling [corrected] is controlled by syntenin-PIP2 interaction and Arf6.* Dev Cell, 2005. **9**(3): p. 377-88.

60. Hongu, T., et al., *Arf6 regulates tumour angiogenesis and growth through HGF-induced endothelial β1 integrin recycling.* Nat Commun, 2015. **6**: p. 7925.

61. Hashimoto, S., et al., *Requirement for Arf6 in breast cancer invasive activities.* Proc Natl Acad Sci U S A, 2004. **101**(17): p. 6647-52.

62. Muralidharan-Chari, V., et al., *ARF6-regulated shedding of tumor cell-derived plasma membrane microvesicles.* Curr Biol, 2009. **19**(22): p. 1875-85.

63. Muralidharan-Chari, V., et al., *ADP-ribosylation factor 6 regulates tumorigenic and invasive properties in vivo.* Cancer Res, 2009. **69**(6): p. 2201-9.

64. Yang, C.Z. and M. Mueckler, *ADP-ribosylation factor 6 (ARF6) defines two insulin-regulated secretory pathways in adipocytes.* J Biol Chem, 1999. **274**(36): p.

25297-300.

65. Aikawa, Y. and T.F. Martin, *ARF6 regulates a plasma membrane pool of phosphatidylinositol(4,5)bisphosphate required for regulated exocytosis.* J Cell Biol, 2003. **162**(4): p. 647-59.

66. Caumont, A.S., et al., *Identification of a plasma membrane-associated guanine nucleotide exchange factor for ARF6 in chromaffin cells. Possible role in the regulated exocytotic pathway.* J Biol Chem, 2000. **275**(21): p. 15637-44.

67. Lawrence, J.T. and M.J. Birnbaum, *ADP-ribosylation factor 6 regulates insulin secretion through plasma membrane phosphatidylinositol 4,5-bisphosphate.* Proc Natl Acad Sci U S A, 2003. **100**(23): p. 13320-5.

68. Santy, L.C., K.S. Ravichandran, and J.E. Casanova, *The DOCK180/Elmo complex couples ARNO-mediated Arf6 activation to the downstream activation of Rac1.* Curr Biol, 2005. **15**(19): p. 1749-54.

69. Koo, T.H., B.A. Eipper, and J.G. Donaldson, *Arf6 recruits the Rac GEF Kalirin to the plasma membrane facilitating Rac activation.* BMC Cell Biol, 2007. **8**: p. 29.

70. Zhang, Q., et al., *A requirement for ARF6 in Fcγ receptor-mediated phagocytosis in macrophages.* J Biol Chem, 1998. **273**(32): p. 19977-81.

71. Niedergang, F., et al., *ADP ribosylation factor 6 is activated and controls membrane delivery during phagocytosis in macrophages.* J Cell Biol, 2003. **161**(6): p. 1143-50.

72. Wong, K.W. and R.R. Isberg, *Arf6 and phosphoinositol-4-phosphate-5-kinase activities permit bypass of the Rac1 requirement for β1 integrin-mediated bacterial uptake.* J Exp Med, 2003. **198**(4): p. 603-14.

73. Balana, M.E., et al., *ARF6 GTPase controls bacterial invasion by actin remodelling.* J Cell Sci, 2005. **118**(Pt 10): p. 2201-10.

74. Uchida, H., et al., *PAG3/Papalpha/KIAA0400, a GTPase-activating protein for ADP-ribosylation factor (ARF), regulates ARF6 in Fcγ receptor-mediated phagocytosis of macrophages.* J Exp Med, 2001. **193**(8): p. 955-66.

75. Swanson, J.A. and C. Watts, *Macropinocytosis.* Trends Cell Biol, 1995. **5**(11): p. 424-8.

76. Cardelli, J., *Phagocytosis and macropinocytosis in Dictyostelium: phosphoinositide-based processes, biochemically distinct.* Traffic, 2001. **2**(5): p. 311-20.

77. Amyere, M., et al., *Origin, originality, functions, subversions and molecular signalling of macropinocytosis.* Int J Med Microbiol, 2002. **291**(6-7): p. 487-94.

78. Bernards, A., *GAPs galore! A survey of putative Ras superfamily GTPase activating proteins in man and Drosophila.* Biochim Biophys Acta, 2003. **1603**(2): p. 47-82.

79. Frittoli, E., et al., *The primate-specific protein TBC1D3 is required for optimal macropinocytosis in a novel ARF6-dependent pathway.* Mol Biol Cell, 2008. **19**(4): p. 1304-16.

80. Ikeda, S., et al., *Novel role of ARF6 in vascular endothelial growth factor-induced signaling and angiogenesis.* Circ Res, 2005. **96**(4): p. 467-75.

81. Schweitzer, J.K. and C. D'Souza-Schorey, *Localization and activation of the ARF6 GTPase during cleavage furrow ingression and cytokinesis.* J Biol Chem, 2002. **277**(30): p. 27210-6.

82. Shan, X.W., et al., *[Small RNA interference-mediated ADP-ribosylation factor 6 silencing inhibits proliferation, migration and invasion of human prostate cancer PC-3 cells].* Nan Fang Yi Ke Da Xue Xue Bao, 2016. **36**(6): p. 735-43.

83. Knizhnik, A.V., et al., *Arf6 promotes cell proliferation via the PLD-mTORC1 and p38MAPK pathways.* J Cell Biochem, 2012. **113**(1): p. 360-71.

84.   Li, M., et al., *Adenosine diphosphate-ribosylation factor 6 is required for epidermal growth factor-induced glioblastoma cell proliferation.* Cancer, 2009. **115**(21): p. 4959-72.

85.   Chabu, C., D.M. Li, and T. Xu, *EGFR/ARF6 regulation of Hh signalling stimulates oncogenic Ras tumour overgrowth.* Nat Commun, 2017. **8**: p. 14688.

86.   Rueckert, C. and V. Haucke, *The oncogenic TBC domain protein USP6/TRE17 regulates cell migration and cytokinesis.* Biol Cell, 2012. **104**(1): p. 22-33.

87.   Yoo, J.H., et al., *ARF6 Is an Actionable Node that Orchestrates Oncogenic GNAQ Signaling in Uveal Melanoma.* Cancer Cell, 2016. **29**(6): p. 889-904.

88.   Suzuki, T., et al., *Crucial role of the small GTPase ARF6 in hepatic cord formation during liver development.* Mol Cell Biol, 2006. **26**(16): p. 6149-56.

89.   Miura, Y., et al., *The small G protein Arf6 expressed in keratinocytes by HGF stimulation is a regulator for skin wound healing.* Sci Rep, 2017. **7**: p. 46649.

90.   Akiyama, M., et al., *Trans-regulation of oligodendrocyte myelination by neurons through small GTPase Arf6-regulated secretion of fibroblast growth factor-2.* Nat Commun, 2014. **5**: p. 4744.

91.   Huang, Y., et al., *Arf6 controls platelet spreading and clot retraction via integrin $α_{IIb}β_3$ trafficking.* Blood, 2016. **127**(11): p. 1459-67.

92.   Tammela, T. and K. Alitalo, *Lymphangiogenesis: Molecular mechanisms and future promise.* Cell, 2010. **140**(4): p. 460-76.

93.   Wigle, J.T. and G. Oliver, *Prox1 function is required for the development of the murine lymphatic system.* Cell, 1999. **98**(6): p. 769-78.

94.   Srinivasan, R.S., et al., *Lineage tracing demonstrates the venous origin of the mammalian lymphatic vasculature.* Genes Dev, 2007. **21**(19): p. 2422-32.

95.   Francois, M., et al., *Segmental territories along the cardinal veins generate lymph sacs via a ballooning mechanism during embryonic lymphangiogenesis in mice.* Dev Biol, 2012. **364**(2): p. 89-98.

96.   Yang, Y., et al., *Lymphatic endothelial progenitors bud from the cardinal vein and intersomitic vessels in mammalian embryos.* Blood, 2012. **120**(11): p. 2340-8.

97.   Karkkainen, M.J., et al., *Vascular endothelial growth factor C is required for sprouting of the first lymphatic vessels from embryonic veins.* Nat Immunol, 2004. **5**(1): p. 74-80.

98.   Yuan, L., et al., *Abnormal lymphatic vessel development in neuropilin 2 mutant mice.* Development, 2002. **129**(20): p. 4797-806.

99.   Wang, Y., et al., *Ephrin-B2 controls VEGF-induced angiogenesis and lymphangiogenesis.* Nature, 2010. **465**(7297): p. 483-6.

100.   Galvagni, F., et al., *Endothelial cell adhesion to the extracellular matrix induces c-Src-dependent VEGFR-3 phosphorylation without the activation of the receptor intrinsic kinase activity.* Circ Res, 2010. **106**(12): p. 1839-48.

101.   Tammela, T., et al., *VEGFR-3 controls tip to stalk conversion at vessel fusion sites by reinforcing Notch signalling.* Nat Cell Biol, 2011. **13**(10): p. 1202-13.

102.   Planas-Paz, L., et al., *Mechanoinduction of lymph vessel expansion.* EMBO J, 2012. **31**(4): p. 788-804.

103.   Breiteneder-Geleff, S., et al., *[Podoplanin--a specific marker for lymphatic endothelium expressed in angiosarcoma].* Verh Dtsch Ges Pathol, 1999. **83**: p. 270-5.

104.   Schacht, V., et al., *T1α/podoplanin deficiency disrupts normal lymphatic vasculature formation and causes lymphedema.* EMBO J, 2003. **22**(14): p. 3546-56.

105.   Suzuki-Inoue, K., et al., *A novel Syk-dependent mechanism of platelet activation by the C-type lectin receptor CLEC-2.* Blood, 2006. **107**(2): p. 542-9.

106. Suzuki-Inoue, K., et al., *Involvement of the snake toxin receptor CLEC-2, in podoplanin-mediated platelet activation, by cancer cells.* J Biol Chem, 2007. **282**(36): p. 25993-6001.

107. Uhrin, P., et al., *Novel function for blood platelets and podoplanin in developmental separation of blood and lymphatic circulation.* Blood, 2010. **115**(19): p. 3997-4005.

108. Norrmen, C., et al., *FOXC2 controls formation and maturation of lymphatic collecting vessels through cooperation with NFATc1.* J Cell Biol, 2009. **185**(3): p. 439-57.

109. Achen, M.G., B.K. McColl, and S.A. Stacker, *Focus on lymphangiogenesis in tumor metastasis.* Cancer Cell, 2005. **7**(2): p. 121-7.

110. Kyzas, P.A., et al., *Evidence for lymphangiogenesis and its prognostic implications in head and neck squamous cell carcinoma.* J Pathol, 2005. **206**(2): p. 170-7.

111. Neuchrist, C., et al., *Vascular endothelial growth factor C and vascular endothelial growth factor receptor 3 expression in squamous cell carcinomas of the head and neck.* Head Neck, 2003. **25**(6): p. 464-74.

112. Mohammed, R.A., et al., *Prognostic significance of vascular endothelial cell growth factors -A, -C and -D in breast cancer and their relationship with angio- and lymphangiogenesis.* Br J Cancer, 2007. **96**(7): p. 1092-100.

113. Schoppmann, S.F., et al., *VEGF-C expressing tumor-associated macrophages in lymph node positive breast cancer: impact on lymphangiogenesis and survival.* Surgery, 2006. **139**(6): p. 839-46.

114. Wartiovaara, U., et al., *Peripheral blood platelets express VEGF-C and VEGF which are released during platelet activation.* Thromb Haemost, 1998. **80**(1): p. 171-5.

115. Alitalo, K., T. Tammela, and T.V. Petrova, *Lymphangiogenesis in development and human disease.* Nature, 2005. **438**(7070): p. 946-53.

116. Joyce, J.A. and J.W. Pollard, *Microenvironmental regulation of metastasis.* Nat Rev Cancer, 2009. **9**(4): p. 239-52.

117. Tobler, N.E. and M. Detmar, *Tumor and lymph node lymphangiogenesis--impact on cancer metastasis.* J Leukoc Biol, 2006. **80**(4): p. 691-6.

118. He, Y., et al., *Suppression of tumor lymphangiogenesis and lymph node metastasis by blocking vascular endothelial growth factor receptor 3 signaling.* J Natl Cancer Inst, 2002. **94**(11): p. 819-25.

119. Karpanen, T., et al., *Vascular endothelial growth factor C promotes tumor lymphangiogenesis and intralymphatic tumor growth.* Cancer Res, 2001. **61**(5): p. 1786-90.

120. Shimizu, K., et al., *Suppression of VEGFR-3 signaling inhibits lymph node metastasis in gastric cancer.* Cancer Sci, 2004. **95**(4): p. 328-33.

121. Roberts, N., et al., *Inhibition of VEGFR-3 activation with the antagonistic antibody more potently suppresses lymph node and distant metastases than inactivation of VEGFR-2.* Cancer Res, 2006. **66**(5): p. 2650-7.

122. Caunt, M., et al., *Blocking neuropilin-2 function inhibits tumor cell metastasis.* Cancer Cell, 2008. **13**(4): p. 331-42.

123. Brice, G., et al., *Milroy disease and the VEGFR-3 mutation phenotype.* J Med Genet, 2005. **42**(2): p. 98-102.

124. Gordon, K., et al., *Mutation in vascular endothelial growth factor-C, a ligand for vascular endothelial growth factor receptor-3, is associated with autosomal dominant milroy-like primary lymphedema.* Circ Res, 2013. **112**(6): p. 956-60.

125. Irrthum, A., et al., *Mutations in the transcription factor gene SOX18 underlie recessive and dominant forms of hypotrichosis-lymphedema-telangiectasia.* Am J Hum Genet, 2003. **72**(6): p. 1470-8.

126. Francois, M., et al., *Sox18 induces development of the lymphatic vasculature in mice.* Nature, 2008. **456**(7222): p. 643-7.

127. Alders, M., et al., *Mutations in CCBE1 cause generalized lymph vessel dysplasia in humans.* Nat Genet, 2009. **41**(12): p. 1272-4.

128. Hogan, B.M., et al., *Ccbe1 is required for embryonic lymphangiogenesis and venous sprouting.* Nat Genet, 2009. **41**(4): p. 396-8.

129. Vreeburg, M., et al., *Lymphedema-distichiasis syndrome: a distinct type of primary lymphedema caused by mutations in the FOXC2 gene.* Int J Dermatol, 2008. **47 Suppl 1**: p. 52-5.

130. Koltowska, K., et al., *Getting out and about: the emergence and morphogenesis of the vertebrate lymphatic vasculature.* Development, 2013. **140**(9): p. 1857-70.

131. Hasegawa, Y., et al., *Novel ROSA26 Cre-reporter knock-in C57BL/6N mice exhibiting green emission before and red emission after Cre-mediated recombination.* Exp Anim, 2013. **62**(4): p. 295-304.

132. Hasegawa, Y., et al., *Generation and characterization of Ins1-cre-driver C57BL/6N for exclusive pancreatic beta cell-specific Cre-loxP recombination.* Exp Anim, 2014. **63**(2): p. 183-91.

133. Kazenwadel, J., et al., *In vitro assays using primary embryonic mouse lymphatic endothelial cells uncover key roles for FGFR1 signalling in lymphangiogenesis.* PLoS One, 2012. **7**(7): p. e40497.

134. Akiyama, M., et al., *Tissue- and development-dependent expression of the small GTPase Arf6 in mice.* Dev Dyn, 2010. **239**(12): p. 3416-35.

135. James, J.M., A. Nalbandian, and Y.S. Mukouyama, *TGFβ signaling is required for sprouting lymphangiogenesis during lymphatic network development in the skin.* Development, 2013. **140**(18): p. 3903-14.

136. Coxam, B., et al., *Pkd1 regulates lymphatic vascular morphogenesis during development.* Cell Rep, 2014. **7**(3): p. 623-33.

137. Outeda, P., et al., *Polycystin signaling is required for directed endothelial cell migration and lymphatic development.* Cell Rep, 2014. **7**(3): p. 634-44.

138. Kukk, E., et al., *VEGF-C receptor binding and pattern of expression with VEGFR-3 suggests a role in lymphatic vascular development.* Development, 1996. **122**(12): p. 3829-37.

139. Joukov, V., et al., *A novel vascular endothelial growth factor, VEGF-C, is a ligand for the Flt4 (VEGFR-3) and KDR (VEGFR-2) receptor tyrosine kinases.* EMBO J, 1996. **15**(2): p. 290-98.

140. Etienne-Manneville, S. and A. Hall, *Integrin-mediated activation of Cdc42 controls cell polarity in migrating astrocytes through PKCζ.* Cell, 2001. **106**(4): p. 489-98.

141. Cox, E.A., S.K. Sastry, and A. Huttenlocher, *Integrin-mediated adhesion regulates cell polarity and membrane protrusion through the Rho family of GTPases.* Mol Biol Cell, 2001. **12**(2): p. 265-77.

142. Zovein, A.C., et al., *Beta1 integrin establishes endothelial cell polarity and arteriolar lumen formation via a Par3-dependent mechanism.* Dev Cell, 2010. **18**(1): p. 39-51.

143. Shafaq-Zadah, M., et al., *Persistent cell migration and adhesion rely on retrograde transport of β(1) integrin.* Nat Cell Biol, 2016. **18**(1): p. 54-64.

144. Dunphy, J.L., et al., *The Arf6 GEF GEP100/BRAG2 regulates cell adhesion by controlling endocytosis of β1 integrins.* Curr Biol, 2006. **16**(3): p. 315-20.

145. Chen, P.W., et al., *The Arf6 GTPase-activating proteins ARAP2 and ACAP1 define distinct endosomal compartments that regulate integrin α5β1 traffic.* J Biol Chem, 2014. **289**(44): p. 30237-48.

146. Cao, Y., *Opinion: emerging mechanisms of tumour lymphangiogenesis and lymphatic metastasis.* Nat Rev Cancer, 2005. **5**(9): p. 735-43.

147. Schulte-Merker, S., A. Sabine, and T.V. Petrova, *Lymphatic vascular morphogenesis in development, physiology, and disease.* J Cell Biol, 2011. **193**(4): p. 607-18.

148. Morgan, M.R., et al., *Syndecan-4 phosphorylation is a control point for integrin recycling.* Dev Cell, 2013. **24**(5): p. 472-85.

149. Okada, R., et al., *Activation of the Small G Protein Arf6 by Dynamin2 through Guanine Nucleotide Exchange Factors in Endocytosis.* Sci Rep, 2015. **5**: p. 14919.

150. Lassing, I. and U. Lindberg, *Specific interaction between phosphatidylinositol 4,5-bisphosphate and profilactin.* Nature, 1985. **314**(6010): p. 472-4.

151. Janmey, P.A. and T.P. Stossel, *Modulation of gelsolin function by phosphatidylinositol 4,5-bisphosphate.* Nature, 1987. **325**(6102): p. 362-4.

152. Fukami, K., et al., *Requirement of phosphatidylinositol 4,5-bisphosphate for α-actinin function.* Nature, 1992. **359**(6391): p. 150-2.

153. Melendez, A.J., M.M. Harnett, and J.M. Allen, *Crosstalk between ARF6 and protein kinase Cα in FcγRI-mediated activation of phospholipase D1.* Curr Biol, 2001. **11**(11): p. 869-74.

154. Powner, D.J., M.N. Hodgkin, and M.J. Wakelam, *Antigen-stimulated activation of phospholipase D1b by Rac1, ARF6, and PKCα in RBL-2H3 cells.* Mol Biol Cell, 2002. **13**(4): p. 1252-62.

155. Kooijman, E.E., et al., *Modulation of membrane curvature by phosphatidic acid and lysophosphatidic acid.* Traffic, 2003. **4**(3): p. 162-74.

156. McMahon, H.T. and J.L. Gallop, *Membrane curvature and mechanisms of dynamic cell membrane remodelling.* Nature, 2005. **438**(7068): p. 590-6.

157. van den Bout, I. and N. Divecha, *PIP5K-driven PtdIns(4,5)P2 synthesis: regulation and cellular functions.* J Cell Sci, 2009. **122**(Pt 21): p. 3837-50.

158. Nishimura, T. and K. Kaibuchi, *Numb controls integrin endocytosis for directional cell migration with aPKC and PAR-3.* Dev Cell, 2007. **13**(1): p. 15-28.

159. Kartopawiro, J., et al., *Arap3 is dysregulated in a mouse model of hypotrichosis-lymphedema-telangiectasia and regulates lymphatic vascular development.* Hum Mol Genet, 2014. **23**(5): p. 1286-97.

160. Miura, Y., et al., *ACAP3 regulates neurite outgrowth through its GAP activity specific to Arf6 in mouse hippocampal neurons.* Biochem J, 2016. **473**(17): p. 2591-602.

161. Sabin, F.R., *On the origin of the lymphatic system from the veins and the development of the lymph hearts and thoracic duct in the pig.* American Journal of Anatomy, 1902. **1**(3): p. 367-389.

162. Martinez-Corral, I., et al., *Nonvenous origin of dermal lymphatic vasculature.* Circ Res, 2015. **116**(10): p. 1649-54.

163. Paez-Ribes, M., et al., *Antiangiogenic therapy elicits malignant progression of tumors to increased local invasion and distant metastasis.* Cancer Cell, 2009. **15**(3): p. 220-31.

164. Ebos, J.M., et al., *Accelerated metastasis after short-term treatment with a potent inhibitor of tumor angiogenesis.* Cancer Cell, 2009. **15**(3): p. 232-9.

Acknowledgements